Time-Resolved Vibrational Spectroscopy of Electronically Excited Inorganic Complexes in Solution

Jon R. Schoonover*

Chemical Science and Technology Division, Mail Stop J586, Los Alamos National Laboratory, Los Alamos, New Mexico 87545

Geoffrey F. Strouse

Department of Chemistry, University of California—Santa Barbara, Santa Barbara, California 93106

Received December 10, 1996 (Revised Manuscript Received February 10, 1998)

Contents

I. Introduction

Time-resolved vibrational spectroscopic studies of electronic excited states in solution were reviewed by Morris and Woodruff in 1987.[1] This review focused on time-resolved resonance Raman (TR^3) experiments. While these efforts continue to be vital, transient Raman spectroscopy, and more recently transient infrared spectroscopy, are being increasingly applied to molecular assemblies to study the intermediate excited states formed following photoinduced electron or energy transfer. The ability to obtain structural information following the absorption of a photon is an important component of photochemical and photophysical research, which includes research related to artificial photosynthesis, photoinitiated reactions, energy transduction, energy conversion, photocatalysis, and photoremediation.

Time-resolved infrared (TRIR) spectroscopy complements the Raman method, and with the advances made recently in TRIR spectroscopy, infrared spectra can now be measured on the time scales previously obtained only by the transient Raman method. This technique is particularly valuable in, but not limited to, the study of metal complexes containing CO or CN^-. These ligands are useful because the ν(CO) and ν(CN) bands have large oscillator strengths and the sensitivities of their frequencies and bandwidths to electronic and molecular structure are well established. Electronic excitation generally produces transient changes in the infrared absorption that are characteristic of the changes in electron density within the complex. A potentially valuable approach to transient infrared studies of excited states on the nanosecond time scale uses step-scan interferometry. This approach has the ability to supply vibrational information throughout the middle-infrared region.[2] Some studies utilizing time-resolved infrared spectroscopy of excited states of transition-metal complexes have been reviewed by Turner and Ford.[3]

* Author to whom correspondence should be addressed.

S0009-2665(95)00273-1 CCC: $30.00
Published on Web 04/28/1998

Jon R. Schoonover was born in Reedsburg, WI, in 1959. He received a B.S. degree in Chemistry from Hampden-Sydney College in Virginia in 1981 and a Ph.D. in Analytical Chemistry from The University of Texas at Austin in 1986, working with W. H. Woodruff. Following postdoctoral fellowships with G. A. Palmer at Rice University and T. J. Meyer at the University of North Carolina at Chapel Hill, Dr. Schoonover joined Los Alamos National Laboratory as a technical staff member in 1993. He is currently part of the Chemical Science and Technology Division at Los Alamos. His research has focused on the development and application of vibrational spectroscopy with the goal of understanding complex chemical problems. This includes studies involving time-resolved vibrational spectroscopy and, more recently, vibrational microspectroscopy and imaging. E-mail: schoons@lanl.gov.

Geoffrey F. Strouse was born in Baltimore, MD, in 1965. He received a B.S. degree in Chemistry from Davidson College in North Carolina in 1987 and a Ph.D. in Inorganic Chemistry from The University of North Carolina at Chapel Hill in 1993, working with Thomas J. Meyer. Following postdoctoral fellowships with Hans U. Guedel at the University of Bern, Switzerland, and Basil I. Swanson at Los Alamos National Laboratory, Dr. Strouse joined the Department of Chemistry at the University of California—Santa Barbara as an Assistant Professor in 1997. His research has focused on the synthesis and spectroscopy of nanoscale soft condensed phase materials directed toward the development of molecular level ion transport and magneto- and electrooptic devices. His research addresses issues involving the complex interplay of crystallographic, electronic, and magnetic properties on local structure in soft-phase materials. This includes mesoscale structural studies on metal-backbone liquid crystalline materials, quantized semiconductors, and transmembrane biomaterials in nanoporous oxide membranes. E-mail: Strouse@chem.ucsb.edu.

This review focuses on the characterization of excited states following electronic excitation in solution using TR[3] and/or TRIR spectroscopies. These methods have been used extensively to monitor photodissociation reactions and to study organic (polyene, polyacene, and heterocyclic) and biological (bacteriorhodopsin, heme protein, and porphyrin) systems; however, this review focuses on electronically excited states of inorganic complexes. The review encompasses the rapid growth of research from 1986 to 1996 and is organized according to structural similarities of the molecules studied. Every effort has been made to be comprehensive in reviewing the many reports in this area. This review is organized into five sections. Section I is the introduction. In section II, an abbreviated background on vibrational spectroscopy and the photophysics of inorganic systems is given; more in-depth treatments of these two topics should be sought elsewhere. Section III provides a general description of the instrumentation used. This section gives only a few experimental approaches without any detailed mention of the wide variety of laser and detection systems used to perform time-resolved vibrational spectroscopy. Section IV focuses on transient vibrational studies of transition-metal complexes, and section V considers studies of polynuclear (supramolecular) systems and molecular assemblies.

II. Vibrational Spectroscopy and Inorganic Photophysics

A. Vibrational Spectroscopy

Molecules are dynamic systems that interact with external fields. These interactions generate electronic absorptions, molecular translations, molecular vibrations, and molecular rotations. For a given molecule, there are $3N$ degrees of freedom, of which 6 degrees of freedom involve molecular rotations and translations. The remaining, $3N$-6, degrees of freedom are the normal vibrational modes for the molecule. These molecular vibrations can result in either changes in the molecular dipole moment (infrared active) or changes in the polarizability of a bond (Raman active). Infrared spectroscopy is a direct absorption measurement of the change in the dipole moment. Raman spectroscopy measures changes in polarizability and is an inelastic scattering measurement. The vibrational bands observed in a Raman or IR spectrum are dictated by selection rules and group theoretical considerations of symmetry for the molecule.

Electronic excitation of a molecule alters the spatial distribution of the electron density, which results in changes in the vibronic structure. The same considerations for the vibrational bands apply to molecules in the excited state. In the excited state, relative to the ground state, shifts to higher and/or lower energy are observed for the vibrational bands on the time scale of the excited-state lifetime. These shifts can be interpreted in terms of structural or electronic changes in the excited-state molecule, providing significant insight into its transient structure.

It should be noted that the observed vibrational bands for complex systems are not simple vibrations of the molecule but a linear combination of normal modes that are generally different for the ground and excited states. To fully interpret the excited-state and ground-state spectra, a full normal-coordinate analysis is required.

In transient Raman spectroscopy, the laser pulse width greatly affects the experimental resolution in the excited-state spectrum. Due to the uncertainty principle, the shorter the pulse width is in time, the broader the pulse is in frequency. Thus, time-resolved vibrational spectroscopy in the femtosecond regime is extremely difficult because of pulse broadening in the frequency domain.

The ability to measure transient Raman signals depends on the resonance Raman (RR) effect. The resonance effect produces large enhancements of the intensities of Raman signals when the wavelength of the incident light is near an electronic absorption band of the sample. Increases in Raman intensity of 4−6 orders of magnitudes are possible. Resonance Raman scattering provides an extremely sensitive and selective probe for dilute transient species. The basis of the resonance Raman effect is briefly given below.

The intensity of Raman scattering is given by

$$I(\nu_r) = (\text{constant})\nu_r^4 I(\nu_0)\sum_{\rho\sigma}|R_{\rho\sigma}|^2 \qquad (1)$$

and

$$R_{\rho\sigma} = \alpha_{\rho\sigma}\mathbf{E} \qquad (2)$$

where ν_0 is the frequency of incident light; ν_r is the Raman frequency; ρ and σ are the x, y, or z components; and $\alpha_{\rho\sigma}$ is the ρth, σth element of the polarizability tensor. A quantum mechanical treatment of the Raman polarizability tensor provides an expression for the intensity of Raman scattering that accounts for resonance enhancement. A second-order perturbation theory calculation of polarizability gives

$$(\alpha_{\rho\sigma})_{gf} = \sum_e \left[\frac{\langle f|\mu_\rho|e\rangle\langle e|\mu_\sigma|g\rangle}{(\nu_{ge} - \nu_0 + i\Gamma_e)} + \frac{\langle f|\mu_\sigma|g\rangle\langle e|\mu_\rho|g\rangle}{(\nu_{ef} - \nu_0 + i\Gamma_e)}\right] \qquad (3)$$

where g and f are the initial- and final-state wave functions, and μ_ρ and μ_σ are the dipole moment operators. The wave function of an intermediate state is e; ν_{ge} and ν_{ef} are transition frequencies from g to e and e to f, $\nu_0 = \nu_{laser}$, and $i\Gamma_e$ is a damping factor.[4−6] In resonance Raman scattering (ν_0 approaching ν_{ge}), the first term of the expression dominates and is responsible for the resonance effect.

A useful alternative theoretical description of the RR process has been derived by Heller.[7] The Heller theory is essentially a time-domain approach which exploits the fact that Raman scattering is a short time-scale process, occurring in a small fraction of the period of a molecular vibration. There is, therefore, no need to know the eigenstates of the excited electronic state because there is insufficient time for these eigenstates to be resolved. The advantage of this theory is in its use of wave packet dynamics, which allow for Raman intensities to be viewed as the result of a classical force exerted by the excited-state potential surface at the equilibrium nuclear coordinate of the ground state (Franck−Condon region). This description stresses the temporal evolution of the scattering process and results in a more realistic and practical guide for the interpretation of RR intensities.

B. Excited-State Processes in Transition-Metal Coordination Complexes

The excited-state properties of transition-metal coordination complexes traditionally have been studied by optical spectroscopy (UV−visible absorption and emission) and can be described as arising from (1) metal-to-ligand charge transfer (MLCT), (2) ligand-to-metal charge transfer (LMCT), or (3) ligand-centered (LC) or (4) ligand-field (LF) excited states. In some cases, the excited-state behavior is more complex, and it is apparent that dual or mixed excited-state processes must be invoked. The observed photochemical and photophysical events are directly correlated to the lowest-lying excited state for these molecules. As an illustration, we describe the photophysics of a single-coordination compound, *fac*-[Re(bpy)(CO)$_3$(4-Etpy)]$^+$. (In this compound bpy is 2,2′-bipyridine and 4-Etpy is 4-ethylpyridine.)

For *fac*-[Re(bpy)(CO)$_3$(4-Etpy)]$^+$, as well as numerous other low-spin d^6 transition-metal complexes, the lowest-lying excited state is MLCT-based (see Scheme 1). This transition involves the promotion of an electron from a Re(I) dπ orbital to the π^* orbital on the bipyridine ligand resulting in an excited-state best described as *fac*-[Re^{II}(bpy$^{\cdot-}$)(CO)$_3$(4-Etpy)]$^{+}$*.

Scheme 1

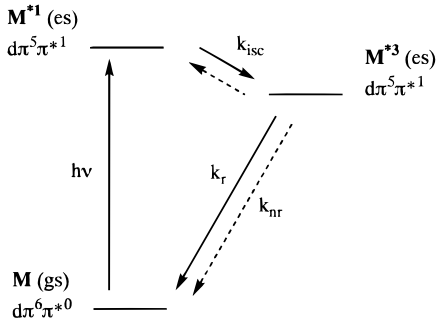

The excited-state lifetime τ for this complex is controlled by the recombination rate of the charge-separated electron and hole and can be described in terms of the nonradiative (vibrational relaxation) rate k_{nr} and the radiative rate k_r:

$$1/\tau = k_{nr} + k_r \qquad (4)$$

(In Scheme 1, k_{isc} is the rate of intersystem crossing.)

For the Re carbonyl complex, the excited-state decay is dominated by the nonradiative pathway. The extent of vibrational overlap between the initial (ground) and final (excited) states determines how much the nonradiative term contributes to the observed excited-state decay. The molecular vibrations involved (acceptor modes) are those in which there is a change in equilibrium displacement or frequency between the initial and final states (see Figure 1). As this distortion increases, the vibrational overlap increases for the acceptor modes, and the contributions from nonradiative terms increase.

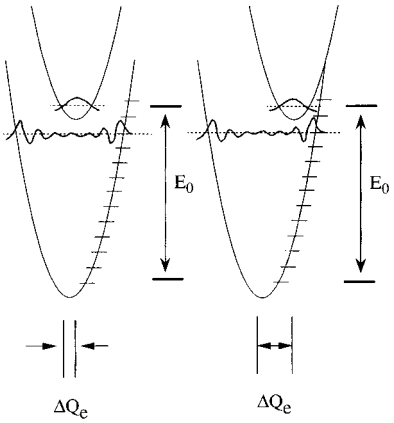

Figure 1. Potential energy diagram illustrating the effect of changes in equilibrium displacement (ΔQ_e) on vibrational wave function overlap.

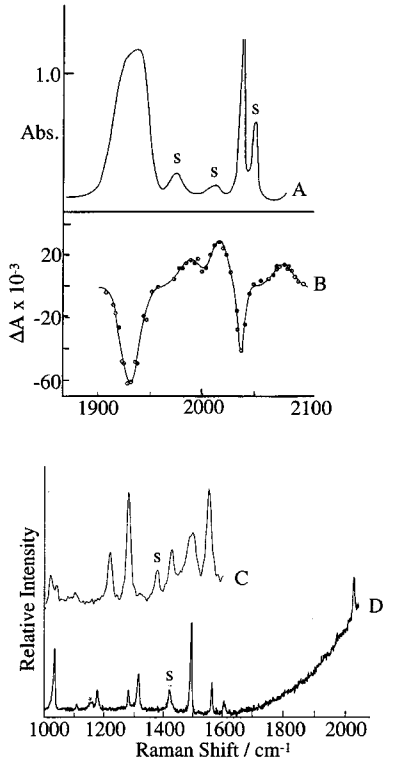

Figure 2. The top portion compares (A) the ground-state FTIR spectrum of *fac*-[Re(bpy)$(CO)_3$(4-Etpy)]$^+$ and (B) the TRIR difference spectrum (ground minus excited state) point by point following 354.7-nm excitation. The bottom portion compares (C) the transient Raman spectrum (354.7-nm pulse probe) of the MLCT excited state of *fac*-[Re(bpy)-$(CO)_3$(4-Etpy)]$^+$ to (D) the ground-state resonance Raman spectrum (λ_{ex} = 406.7 nm). "S" signifies solvent bands.

Relative to the ground state, the *fac*-[Re^{II}($bpy^{\cdot-}$)-$(CO)_3$(4-Etpy)]$^{+}$* excited state has increased electron density at the ligand, altering the bonding in the bpy ligand. This excited state also has decreased electron density at the metal, changing the back-bonding of the CO ligands. The TR^3 experiment probes changes at the bipyridyl ligand, while the TRIR experiment probes changes at the metal by monitoring changes in the ν(CO) bands (see Figure 2). In the ground-state Fourier transform infrared (FTIR) spectrum, two ν(CO) bands are observed, consistent with C_{3v} symmetry. In contrast, the TRIR spectrum has three ν(CO) bands, indicating reduced symmetry in the excited state (C_s symmetry). These latter bands are shifted to higher energies relative to the ground state, suggesting decreased electron density at the metal, which decreases Re−CO back-bonding and increases the triple-bond character of the carbonyls.

The charge-transfer transition to the bpy ligand produces changes in the electron density and the polarizability at the ligand. These changes produce a set of Raman bands for the excited state that differ from those of the ground state (see Figure 2). As predicted for a charge-transfer state, the new Raman bands can be correlated to the Raman bands observed in the bpy radical anion. For the Raman spectra in both the ground and excited states, the system can be treated as a single 2,2′-bipyridine with C_{2v} symmetry. The observed RR bands between 1000 and 1700 cm^{-1} are attributed to a series of totally symmetric (A_1), highly mixed ring vibrations. The ground-state RR, TR^3, FTIR, and TRIR spectra are compared in Figure 2.

III. Instrumentation

A. Time-Resolved Resonance Raman Spectroscopy

The development of time-resolved vibrational spectroscopy has followed advances in laser and detector technology. The early development of TR^3 spectroscopy has been reviewed by Wilbrandt. Many advances in technology have been made since the initial TR^3 experiments.[8]

The development of optical multichannel analyzers (OMAs) and charge-coupled devices (CCDs) has provided the ability to measure a complete Raman spectrum for each laser pulse when the appropriate OMAs and CCDs are coupled to a single spectrograph. A simplified diagram of one approach to TR^3 spectroscopy on the nanosecond time scale is shown in Figure 3.

Single-color experiments are a popular way to measure the TR^3 spectra of inorganic complexes in solution. In these experiments, a single laser pulse is used both to create the excited state and as a source for the Raman scattering. The first part of the pulse excites the sample, and the remaining part is used as the Raman probe. The detector is operated in the gated mode with the timing controlled by a pulse generator. The signal is then integrated over the gate period (typically 50−100 ns), which is centered over the laser pulse. Given this arrangement, it is difficult to obtain a precise value for the time resolution. However, practically the excited states accessible by this approach must have lifetimes of 20 ns or longer, and the resulting spectrum can be considered as an average of the true excited-state resonance Raman spectra over the time period of the gate. The basis for the TR^3 experiment is illustrated in the energy diagrams shown in Figure 4.

Techniques have been developed to produce picosecond and femtosecond pulses for applications in spectroscopy.[9] Transient picosecond Raman spectroscopy has recently become an area of active research. Advances in laser technology (generation

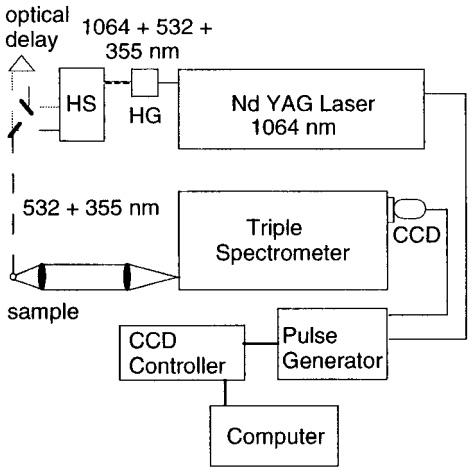

Figure 3. Schematic of a two-color TR[3] experiment with nanosecond time resolution. The source is a Nd:YAG laser which lases at a fundamental wavelength of 1064 nm. The fundamental is frequency doubled and tripled in the harmonic generator (HG) to produce the first (532 nm) and second (354.7 nm) harmonics. These harmonics are separated by the harmonic separator (HS) and the probe wavelength delayed in time relative to the pump wavelength. The Raman scattering is collected and dispersed by a triple spectrometer and detected by a CCD.

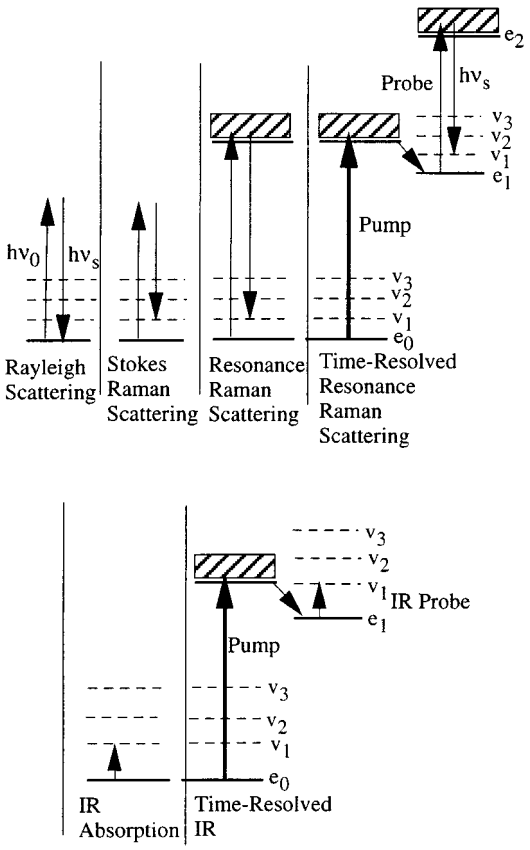

Figure 4. The top portion of the diagram compares Rayleigh scattering, Raman scattering, and resonance Raman scattering to the scattering process in a time-resolved Raman experiment. The bottom portion of the diagram compares ground-state IR absorption to transient IR absorption. The data in this experiment is measured as a difference spectrum:transient IR minus ground-state IR.

of ultrafast pulses with a stable, high repetition rate) and detection systems (such as CCDs) have helped to advance developments in this experimentally challenging area. The first experiments in this area used a single laser pulse, and the transient species was identified by subtracting a lower-power, nonphotolyzed spectrum from the higher-power spectrum.[10] The two-color, pump−probe approach using picosecond laser systems has been demonstrated by several groups.[11] The time resolution in these experiments is determined by the time between the pump and probe pulses. A typical picosecond Raman system is described in ref 12. Ultrafast laser systems make possible elegantly designed experiments to study the very fast processes that follow excitation.

B. Time-Resolved Infrared Spectroscopy

Continuing advances in TRIR spectroscopy make it possible to measure transient IR signals following laser excitation on many time scales (see Figure 4).[2,3,13] One approach to TRIR spectroscopy on the nanosecond time scale uses a monochromatic IR monitoring beam and laser-pulse excitation with transient signals being monitored point by point over the spectral region of interest. The tunable IR light is from either a CO laser (1550−2000 cm^{-1}) or a diode laser (1900−2250 cm^{-1}). It is also possible to obtain transient spectra with a dispersive instrument. Nanosecond time resolution based on a dispersive scanning spectrometer has been achieved.[14] Limitations of this approach include source brightness and the fact that data is measured point by point. These different approaches to nanosecond TRIR have been described and compared elsewhere.[2b]

A potentially valuable approach to nanosecond TRIR spectroscopy, particularly in the study of excited states, uses step-scan FTIR spectroscopy. The advantages of the step-scan FTIR have been well-documented, the main limitation being that the transient event must be repetitively produced during the course of the experiment.[3,15]

Commercial instruments are available for step-scan applications, and these step-scan experiments have recently been extended into the nanosecond time regime.[3c,16,17] In one approach, a commercial system was modified to permit studies of short-lived excited electronic states in solution (see Figure 5). This apparatus uses a step-scan interferometer as the IR source, boxcar integration of a photoconductive mercury cadmium telluride detector, and external optics to tightly focus the IR beam onto the sample and to collect the IR signal. For transient studies of inorganic complexes, efficient pumping of an excited-state process requires tight focusing and careful overlap of the pump and probe beams, preferably in a collinear geometry to minimize photothermal artifacts. Synchronizing the pump laser and the stepping of the interferometer requires external electronics such as a digital delay generator. Allowances must also be made for mechanical settling of the mirror and electronic settling of the detector amplifier.

The pump−probe approach can also be used in TRIR spectroscopy to measure ultrafast IR spectra.[13] One approach to ultrafast IR spectroscopy uses a fast pump pulse and upconversion with a continuous wave (CW) IR signal to produce a second fast visible pulse that can be detected in the visible.[13b−d] This

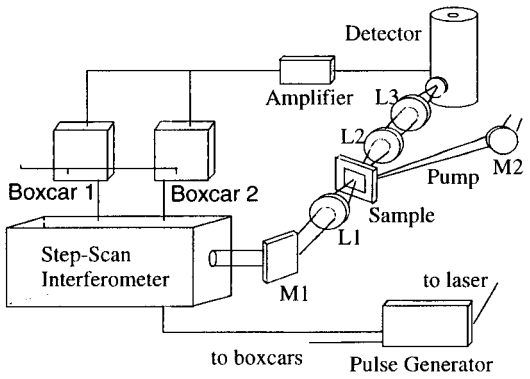

Figure 5. Schematic of the optical arrangement of a step-scan TRIR apparatus with nanosecond time resolution. The system uses a Q-switched Nd:YAG laser (Spectra Physics GCR-11) as the pump source (7 ns, 10 Hz).

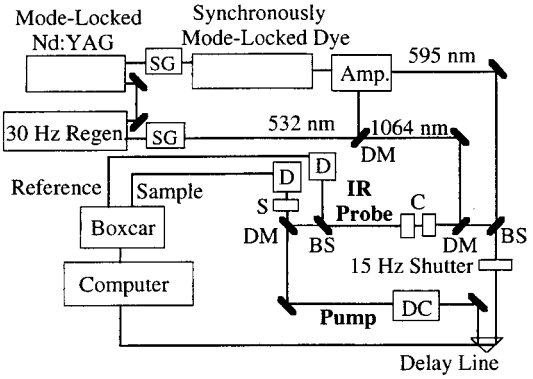

Figure 6. The picosecond TRIR apparatus is based on a pump−probe technique with time resolution obtained by optically delaying (0.3 mm = 1 ps) an infrared probe pulse with respect to a near-UV pump pulse. In the figure: BS = beam splitter, DM = dichroic mirror, D = mercury cadmium telluride detector, SG = second harmonic generator, DC = doubling crystal, C = two nonlinear mixing crystals used to create the IR probe beam, Amp. = dye amplifier train, S = sample.

upconversion experiment is similar in approach to an ultrafast visible transient absorption experiment.

Other experimental approaches use short IR pulses for the probe beam. There are several ways to generate such pulses. In this type of experiment, the probe beam is split into sample and reference beams before reaching the sample and is then interrogated by a mid-IR-sensitive detector. One experimental apparatus for picosecond TRIR measurements is shown in Figure 6.

IV. Electronically Excited States of Transition-Metal Complexes

A. Ruthenium Polypyridyl Complexes

There is an extensive and well-developed excited-state and redox chemistry based on MLCT excited states of polypyridyl complexes of the second and third row ($d\pi^6$) transition-metal ions in solution. Interest in these complexes stems from their photochemical and photophysical properties in solution. These properties include (1) responsiveness to visible light, (2) a long-lived excited state, (3) photochemical stability, (4) enhanced redox properties in the excited state, (5) the ability to undergo facile oxidative and reductive quenching in the excited state, and (6) the extensive synthetic chemistry available.

1. $[Ru(bpy)_3]^{2+}$

The archetypal example of a d^6 polypyridyl complex is tris(bipyridine)ruthenium(II) ($[Ru(bpy)_3]^{2+}$; where bpy is 2,2′-bipyridine). Woodruff et al., followed by Forster and Hester, established that the lowest MLCT excited electronic state of $[Ru(bpy)_3]^{2+}$ can best be characterized as $[Ru^{III}(bpy)_2(bpy^{\cdot-})]^{2+*}$. [4b,18,19] These initial experiments demonstrated the value of TR^3 spectroscopy to determine the structure of short-lived transient species.

The application of TR^3 and RR to $[Ru(bpy)_3]^{2+}$ with isotopically labeled analogues has resulted in calculations of the force fields for the ground state as well as for the anion−radical fragment of the MLCT excited state.[20] The excited-state normal-mode formulations were also derived and compared to those of the ground state. These data strongly supported the original characterization of the lowest MLCT excited state and have supplied a basis for the structural interpretation of TR^3 spectra of $[Ru(bpy)_3]^{2+*}$ and related systems.

2. Mixed Chelates

Additionally, TR^3 spectroscopy allows one to "fingerprint" the excited states of materials. For example, even a slight change in the peripheral substituents on a bpy ligand, e.g., 4,4′-dimethyl-2,2′-bipyridine (dmb) compared to bpy, causes discernibly different resonance Raman spectra. In mixed-ligand or heteroleptic complexes, this difference allows one to determine which ligand acts as the acceptor of the excited electron in the thermally equilibrated excited state. This type of experiment was originally demonstrated by Kincaid et al. as well as by Mabrouk and Wrighton using $[RuL_nL'_{3-n}]^{2+}$ complexes (L, L′ are bpy, dmb, or 4,4′-dibromo-2,2′-bipyridine).[21]

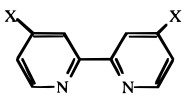

X = -H; bpy

X = $-CH_3$; dmb

X = $-CO_2H$; dcb

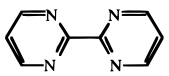

bpm = 2,2'-bipyrimidine

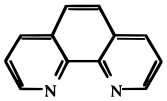

1,10-phenanthroline

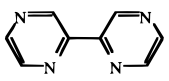

bpz = 2,2'-bipyrazine

In addition to studies of complexes with substituted bpy ligands, experiments have been conducted on a number of complexes using different bidentate polypyridyl ligands. The available synthetic chemistry, coupled with information from RR and TR^3 studies, has opened new possibilities for designing and manipulating specific excited-state properties. Ligand localization of mixed-ligand complexes has been

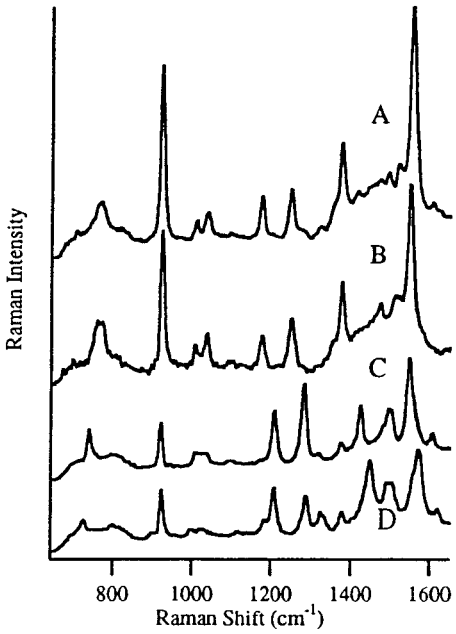

Figure 7. TR^3 spectra (700−1700 cm^{-1}) for (A) $[Ru(bpy)(dmb)(bpm)]^{2+}$, (B) $[Ru(bpm)_3]^{2+}$, (C) $[Ru(dmb)_3]^{2+}$, and (D) $[Ru(bpy)_3]^{2+}$ were measured in degassed CH_3CN at room temperature.

Table 1. Excited-State Resonance Raman Band Energies (cm^{-1}) for $[Ru(bpy)_3]^{2+}$, $[Ru(dmb)_3]^{2+}$, $[Ru(bpm)_3]^{2+}$, and $[Ru(bpy)(dmb)(bpm)]^{2+}$

$[Ru(bpy)_3]^{2+}$	$[Ru(dmb)_3]^{2+}$	$[Ru(bpm)_3]^{2+}$	$[Ru(bpy)(dmb)(bpm)]^{2+}$
1008		1012	1012
	1026		
1029			
		1034	1034
	1177	1174	1174
	1202		
1211			
		1249	1249
1285	1282		
1321	1321		
		1429	1421
1434			
	1445		
		1490	1490
1504	1496		
		1560	1560
1564			
	1572		

studied using the ligands 1,10-phenanthroline, 4,7-diphenyl-1,10-phenanthroline, 4,4′-diphenyl-2,2′-bipyridine, 2,2′-bipyrazine, 4,4′,5,5′-tetramethyl-2,2′-bipyridine, and 2,2′-bipyrimidine together with TR^3 spectra.[22,23,24]

The utility of TR^3 spectroscopy in studying ligand localization is shown in Figure 7 and Table 1, which compare the excited-state spectra of $[Ru(bpy)_3]^{2+*}$, $[Ru(dmb)_3]^{2+*}$, $[Ru(bpm)_3]^{2+*}$, and $[Ru(bpy)(dmb)(bpm)]^{2+*}$ (in these complexes bpm is 2,2′-bipyrimidine). These data were measured in CH_3CN following 354.7-nm excitation (7 ns, 10 Hz) with the same laser pulse used for excitation and as the source for the Raman scattering measurement.[24] The spectra of the homoleptic complexes demonstrate the fingerprinting feature of the Raman approach: considerable differences in Raman shifts and relative intensities are seen in the various spectra. For the heteroleptic complex $[Ru(bpy)(dmb)(bpm)]^{2+}$, the excited-state spectrum lacks the characteristic pattern of bands for $bpy^{\cdot-}$ and $dmb^{\cdot-}$, and Raman bands for $bpm^{\cdot-}$ dominate the spectrum. Formulating the excited state as $[Ru(bpy)(dmb)(bpm^{\cdot-})]^{2+*}$ is consistent with the absence of enhancement from $bpy^{\cdot-}$ and $dmb^{\cdot-}$ bands; the only bpy- or dmb-based bands originate from the ground state.

Nanosecond TR^3 experiments have provided a convincing argument for the localized excited-state model in which localization occurs on the nanosecond time scale. Picosecond TR^3 spectra of $[Ru(bpy)_3]^{2+}$ under a variety of solvent conditions demonstrate that the excited electron is localized on a single bpy ligand within a few picoseconds.[25] In a series of papers, Hopkins's group also investigated electron localization using several different Ru polypyridyl complexes.[26] Two-color picosecond Raman studies were conducted on complexes including $[Ru(bpy)_3]^{2+}$, $[Ru(phen)_3]^{2+}$, $[Ru(bpy)_2(phen)]^{2+}$, $[Ru(phen)_2(bpy)]^{2+}$, $[Ru(bpm)_3]^{2+}$, $[Ru(dcb)_3]^{2+}$, $[Ru(bpm)_2(bpy)]^{2+}$, $[Ru(bpy)_2(bpm)]^{2+}$, and $[Ru(bpy)_2(dcb)]^{2+}$.

TR^3 spectra have also been measured for the MLCT excited state of molecules of the type $[Ru(NH_3)_5L]^{2+}$ (L is 4,4′-bipyridine or 4,4′-bipyridine-H^+).[27] Additionally, some Ru polypyridyl complexes are of interest as molecular probes because their photophysical properties are sensitive to their immediate environment.[28] For example, changes in intensity enhancements and differences in Raman shifts have been noted for TR^3 spectra of $[Ru(bpy)_3]^{2+}$ in anionic micelles.[29] Other complexes are important because of their interactions with nucleic acids.[30] One specific example is the TR^3 study of $[Ru(bpy)_2(dpphen)]^{2+}$ (dpphen is 4,7-diphenyl-1,10-phenanthroline).[31] Initial TR^3 spectra of this complex in water demonstrated features attributed to anion radicals of both bpy and dpphen because the energies of the acceptor levels for the excited electron are very similar for both of these ligands.[22] Further TR^3 studies have shown that in neutral micelles, localization is on bpy, while in the presence of DNA and anionic surfactants, localization is on the dpphen ligand.[31] The excited-state properties of this complex are, therefore, tuned by the solvent conditions. Differences in the solvation conditions of a single complex also provide an opportunity to probe microheterogeneous environments.

3. Characterization of Acceptor Ligands

One exciting application of Ru polypyridyl complexes follows from the observed quenching of the MLCT excited state when associated with DNA, providing insight into DNA structure. One example is $[Ru(phen)_2(dppz)]^{2+}$ (dppz is dipyrido[3,2-*a*:2′,3′-*c*]-phenazine).[32] Complexes that contain more complicated ligands such as dppz as the acceptor ligand offer the possibility of localizing the excited electron within a specific part of the ligand.[33] TR^3 measurements provide a way to establish the structural details of polypyridyl-based ligand systems including inherently asymmetric ligands. The dppz ligand is one example. Initial interpretations of the photophysical properties of $[Ru(bpy)_2(dppz)]^{2+}$ following MLCT excitation suggested that dppz was the accep-

Table 2. Time-Resolved Resonance Raman Studies of MLCT Excited States of $[Ru(bpy)_3]^{2+}$ and Related Complexes

complex	ref(s)	experiment/result
$[Ru(bpy)_3]^{2+}$	4b	original TR^3 study suggesting a MLCT excited-state structure of $[Ru^{III}(bpy)_2(bpy^{\cdot-})]^{2+*}$
$[Ru(bpy)_3]^{2+}$	18	subsequent study by Woodruff et al. with related complexes and radical anion data
$[Ru(bpy)_3]^{2+}$	19	excited-state spectrum of $[Ru(bpy)_3]^{2+*}$ using CW laser excitation
$[Ru(bpy)_3]^{2+}$	20a,b	normal-coordinate analysis of ground and MLCT states of $[Ru(bpy)_3]^{2+}$
$[RuL_nL'_{3-n}]^{2+}$; L, L′ are bpy, dmb, or 4,4′-dibromo-bpy, $n = 0-3$	21a,b	studies of ligand localization in MLCT excited states using mixed-ligand complexes
$[RuL_nL'_{3-n}]^{2+}$; L, L′ are bpy, dpphen, or 4,4′-Ph_2bpy, $n = 0-3$	22a,b	studies of ligand localization in MLCT excited states using mixed-ligand complexes
$[RuL_nL'_{3-n}]^{2+}$; L, L′ are bpy, bpz, or tmb, $n = 0-3$	23a,b,36	studies of ligand localization in MLCT excited states using mixed-ligand complexes
$[RuL_nL'_{3-n}]^{2+}$; L, L′ are bpy, dmb, or bpm, $n = 0-3$	24	studies of ligand localization in MLCT excited states using mixed-ligand complexes; see Table 1
$[Ru(bpy)_3]^{2+}$	25a	picosecond TR^3 study
$[RuL_nL'_{3-n}]^{2+}$; L, L′ are bpy or phen, $n = 0-3$	25b,26a,b	picosecond TR^3 studies of ligand localization in mixed-ligand complexes
$[RuL_nL'_{3-n}]^{2+}$; L, L′ are bpy or bpm, $n = 0-3$		
$[RuL_nL'_{3-n}]^{2+}$; L, L′ are bpy or dcb, $n = 0-3$		
$Ru(NH_3)_5(4,4'\text{-bpy})^{2+}$	27	TR^3 study
$Ru(bpy)_2(dpphen)^{2+}$	31	TR^3 spectra of $Ru(bpy)_2(dpphen)^{2+*}$, demonstrating ligand localization on bpy in neutral micelles and on dpphen in the presence of DNA or anionic surfactants
$[Ru(bpy)_2(dppz)^{2+}$, $Ru(dmb)_2(dppz)]^{2+}$	34	TR^3 studies suggesting localization on dppz with the lowest π^* level on the ligand largely phenazine in character but with some delocalization of the remaining part of the ligand
$[(dmb)_2Ru(\mu\text{-bbpe})Ru(dmb)_2]^{4+}$	35	TR^3 data demonstrate localization on the bppe ligand with delocalization within the ligand over the entire π framework
$[Ru(pypz)_3]^{2+}$, $[Ru(bpy)_2(pypz)]^{2+}$, $[Ru(5\text{-mmb})_3]^{2+}$, $[Ru(5,5'\text{-dmb})_3]^{2+}$, $[Ru(Mebpy)_2]^{2+}$	36,37	TR^3 data demonstrate localization within a specific part of inherently asymmetric ligands

tor ligand but with weak electronic coupling between the bpy and phenazine portions of the ligand.[33] The alternative description is that the excited electron is delocalized in a molecular orbital over the entire ligand framework.

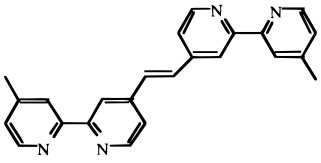

bbpe

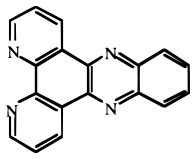

dppz

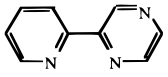

pypz

Comparisons of the RR and TR^3 spectra of $[Ru(bpy)_2(dppz)]^{2+}$ and $[Ru(dmb)_2(dppz)]^{2+}$ (CH_3CN at 298 K) provide insight into the excited-state structure of these complexes.[34] The results demonstrate that the Raman bands are similar to those observed in the electrochemically generated dppz radical anion. The TR^3 spectra can be simulated qualitatively as a combination of bands that are largely phenazine$^{\cdot-}$ and phen$^{\cdot-}$ (representing the two parts of the ligand) in character. This result suggests delocalization over the ligand; the lowest π^* level may be largely phenazine in character but with some delocalization of the excited electron.

Bis(4′-methyl-2,2′-bipyrid-4-yl)ethene, or bbpe, is another large ligand system with interesting photophysical properties. The MLCT excited state of the ligand-bridged complex $[(dmb)_2Ru(\mu\text{-bbpe})Ru(dmb)_2]^{4+}$ has an unusually long excited-state lifetime ($\tau = 1310$ ns in CH_3CN at 298 K, with the emission maximum at 750 nm). The increased lifetime with this ligand is of interest because MLCT lifetimes typically decrease as the emission energy decreases. TR^3 spectra of the bbpe complex show that bbpe is the acceptor ligand following photolysis.[35] There are also insights to be gained from these data regarding the origin of the extended nonradiative lifetime, with evidence that the excited electron is delocalized over the entire bppe skeleton. The data point to the excited electron being delocalized over the large molecular framework, resulting in decreased local bond displacements and a relatively long excited-state lifetime.

Kincaid's group has studied a series of inherently asymmetric polypyridine ligands including Ru complexes containing 2-2-pyridzylpyrazine (pypz), 4-methyl-2,2′-bipyridine, and 5-methyl-2,2′-bipyridine.[36,37] This type of study demands detailed RR and TR^3 studies with the additional aid of isotopically labeled derivatives. In the RR spectra of Ru complexes containing pypz, Raman bands were identified which are assigned to the two different rings of the asymmetric ligand. The TR^3 spectra were interpreted to show polarization of electronic charge toward the pyrizine fragment of the pypz ligand. Similarly, monomethyl substitution at the 4 or 5 position of bpy provides asymmetric charge distribution in the MLCT excited state. This change is caused by the fact that the pyridine fragment can better stabilize the excited electron density. Table 2 lists the TR^3 studies conducted on $[Ru(bpy)_3]^{2+}$ and related complexes.

Table 3. References for Time-Resolved Vibrational Data for Electronically Excited States of Copper Polypyridyl Complexes

complex	ref(s)	study/result
$[Cu(dmp)_2]^+$, $[Cu(dmp)(PPh_3)_2]^+$, $[Cu(dpp)_2]^+$	39−41	data suggesting a localized excited-state structure, $[(L)Cu(L^{\cdot-})]^+$*, following MLCT excitation
$[Cu(DMCH)_2]^+$, $[Cu(BIQ)_2]^+$, $[Cu(DMCH)(PPh_3)_2]^+$, $[Cu(BIQ)(PPh_3)_2]^+$	42	TR^3 and Raman spectroelectrochemical studies investigating neutral and reduced ligand structure in the presence of Cu(I) and Cu(II)

B. Copper Polypyridyl Complexes

A considerable number of time-resolved Raman studies have been conducted on Cu porphyrins, but only the studies concerning copper complexes with polypyridyl ligands are relevant to this review (see Table 3). Cu^I−polypyridine complexes (e.g., $[Cu(phen)_2]^+$) exhibit low-lying MLCT transitions that can participate in electron-transfer processes.[38] Several studies have focused on $[Cu(dmp)_2]^+$ (where dmp is 2,9-dimethyl-1,10-phenanthroline).[39−41] In initial experiments, depletion of ground-state bands was observed, but no features attributable to the ligand radical and the MLCT state were detected. The TR^3 spectrum of the 2,9-diphenyl analogue did show Raman bands indicative of the neutral ligand and the radical anion, which were interpreted as a localized excited state, $[(L)Cu^{II}(L^{\cdot-})]$. Data for complexes with the 2,9-dimethyl ligand suggested a biphotonic process, involving a second long-lived upper excited state with a small scattering cross section. Subsequent time-resolved Raman studies using different probe wavelengths supported the localized model for this complex as well.[41]

Another series of experiments on Cu(I) complexes utilized the parallel application of TR^3 spectroscopy and Raman spectroelectrochemistry.[42] This approach provided a method to study ligand structure (neutral and reduced) in the presence of Cu(I) or Cu(II). A series of bis- and mixed-ligand complexes were studied which used the ligands 2,2′-biquinoline (BIQ), 6,7-dihydro-5,8-dimethyldibenzo[*b*,*j*][1,10]phenanthroline (DMCH), and triphenylphosphine. Raman shifts originating from the MLCT excited state were comparable to shifts from the electrochemically generated radical anions, regardless of the nature of the remaining ligand. One band near 1590 cm^{-1} changed as a function of oxidation state, suggesting that at least one Raman band may be sensitive to the electron density at the metal.

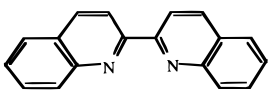

BIQ

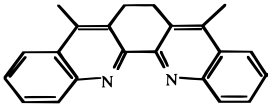

DMCH

C. Metal–Metal Bonded Dimers

1. Quadruple-Bonded Octohalodirhenate Dianions

A class of inorganic molecules whose excited-state structures have been of interest from an experimental, as well as a theoretical, standpoint are metal−metal bonded dimers.[43] One series of molecules studied by TR^3 spectroscopy are the quadruple-bonded octohalodirhenate dianions, $[Re_2X_8]^{2-}$ (where X is Cl, Br, or I). The lowest-lying allowed excited state in the $[Re_2X_8]^{2-}$ complexes is $^1(\delta\rightarrow\delta^*)$ ($^1A_{2u}$), which involves promotion of an electron from a bonding δ orbital to an antibonding δ^* orbital and the concomitant change in metal−metal bond order from 4 to 3. Initial TR^3 data for $[Re_2Cl_8]^{2-}$* suggested an unexpectedly large excited-state shift for the Re−Re symmetric stretch.[44] The RR studies indicated an Re−Re energy of 275 cm^{-1} in the ground state and an excited-state value of 204 cm^{-1}. These values were compared to the 249-cm^{-1} vibronic progression (excited-state Re−Re energy) observed in low-temperature absorption measurements.

Table 4. Comparison of Vibrational Data (cm^{-1}) for the d^8−d^8 Transition Metal Dimers $[Re_2Cl_8]^{2-}$, $[Re_2Br_8]^{2-}$, and $[Mo_2Cl_4(PMe_3)_4]$

dimer	ground-state RR	ground-state vibronic	TR^3	excited-state vibronic	assignment
$[Re_2Br_8]^{2-}$	111		104	98	δ(ReReBr)
	123		126		δ(BrReBr)
	209			216	ν(ReBr)
	275		262	252	ν(ReRe)
$[Re_2Cl_8]^{2-}$	154	158	146	137	δ(ReReCl)
	188		201		δ(ClReCl)
	274	275	262	249	ν(ReRe)
	359		365		ν(ReCl)
$[Mo_2Cl_4(PMe_3)_4]$	355		331	329	ν(MoMo)
	274				ν(MoCl)

Subsequent TR^3 studies of the $\delta\delta^*$ excited states of $[Re_2Cl_8]^{2-}$, $[Re_2Br_8]^{2-}$, and $[Mo_2(PMe_3)_4Cl_4]$ presented a clear picture of the excited-state structure in solution at ambient temperature.[45] The TR^3 spectra of the Re complexes showed bands associated with three symmetrical vibrations: (1) Re−Re stretch, (2) Re−X stretch, and (3) Re−Re−X deformation (see Table 4). A Raman band assigned to the asymmetrical X−Re−X bend was also observed. The data suggests that in solution on the nanosecond time scale the excited-state adopts a staggered configuration with a shorter (0.03−0.04 Å) metal−metal bond distance. In contrast, the vibronic data (low temperature, single crystal) probe the unrelaxed eclipsed structure. This interpretation was confirmed using $[Mo_2(PMe_3)_4Cl_4]$. This complex is precluded by steric effects of the bulky PMe_3 ligands from undergoing significant torsional distortion about the metal−metal bond.

2. d^8–d^8 M_2 Complexes (M = Rh or Pt)

The excited-state structures of d^8−d^8 transition-metal dimers have been studied by TR^3 and TRIR spectroscopy. These complexes possess some inter-

Table 5. Time-Resolved Vibrational Studies of Electronically Excited States of Metal−Metal Bonded Dimers

complex	ref(s)	study/result
$[Re_2Cl_8]^{2-}$, $[Re_2Br_8]^{2-}$, $[Mo_2Cl_4(PMe_3)_4]$	44,45	TR^3 data of $\delta\delta^*$ excited state demonstrating a staggered halide conformation with shortened M−M bond distance for $[Re_2X_8]^{2-*}$
$[Rh_2(b)_4]^{2+}$	47,48	TRIR and TR^3 data demonstrating increased ν(Rh−Rh) and ν(Rh−C) and decreased ν(C−N) frequencies following $d\sigma^*$ to $p\sigma$ excitation
$[Pd_2(dppm)_3]$, $[Pt_2(dppm)_3]$	49	TR^3 studies suggest increased metal−metal bonding in the lowest triplet excited state

esting spectroscopic and photochemical properties.[46] They have a formal metal−metal bond order of zero in the ground state. Optical excitation into the $^1(d\sigma^* \rightarrow p\sigma)$ transition results in rapid, efficient intersystem crossing from the $^1A_{2u}$ state to a long-lived $^3A_{2u}$ ($p\sigma$) state. Initial studies on $[Rh_2b_4]^{2+}$ (where b is 1,3-diisocyanopropane) demonstrated the enhanced metal−metal bonding expected for an excited state arising from the antibonding-to-bonding transition. For $[Rh_2b_4]^{2+*}$, the ground-state Rh−Rh stretch (79 cm^{-1}) shifts to 144 cm^{-1}, and the Rh−C stretch shifts from 467 to 484 cm^{-1}.[47] TRIR measurements show that the ν(CN) band decreases in the excited state from 2193 to 2177 cm^{-1}.[48] This decrease can be rationalized by the increased metal-to-isocyanide back-bonding in the excited state. The increased back-bonding is demonstrated in the shift to higher energy of the ν(Rh−C) band; ν(CN) then decreases because of the additional electron density in an antibonding $2p\pi^*$ orbital on the cyanide. Using the ground- and excited-state Raman band energies, excited-state displacements were calculated: Rh−Rh bond, −0.210 Å; Rh−C bond, −0.022 Å; and CN bond, +0.002 Å.

3. d^{10}–d^{10} M_2 Complexes (M = Pd or Pt)

TR^3 experiments have been used to study metal−metal interactions in the lowest triplet excited states of the d^{10}−d^{10} dimers, $[M_2(dppm)_3]$ [where M is Pd or Pt and dppm is bis(diphenylphosphino)methane].[49] The ν(Pd−Pd) band shifts from the ground-state value of 120 to 152 cm^{-1} in the excited state. Similarly, the ν(Pt−Pt) band shifts from 102 to 120 cm^{-1}. As with the d^8−d^8 dimers, the bonding metal−metal interactions increase in the excited state consistent with the $^3(d\sigma^*p\sigma)$ assignment. The effect is somewhat smaller for the d^{10}−d^{10} systems, with calculated metal−metal displacements of 0.10 Å for $[Pt_2(dppm)_3]$ and 0.12 Å for $[Pd_2(dppm)_3]$. Table 5 lists the various excited-state vibrational studies conducted on metal−metal dimers.

D. Transition-Metal Carbonyl Complexes

Considerable research utilizing time-resolved infrared techniques has focused on metal carbonyl complexes of Re(I), Ru(II), and W(0). Because of strong CO absorption bands in the IR region (1800−2200 cm^{-1}) and the sensitivity of the ν(CO) bands to molecular structure and metal charge, TRIR spectroscopy in the nanosecond time regime is the method of choice to probe the excited-state character of metal carbonyl complexes.[2,16,17] This section concentrates only on studies of the excited states of metal carbonyl complexes in solution, not on the considerable work in the study of photodissociation reactions, gas-phase photochemistry, and CO photolysis and binding in biological systems.

The excited-state properties of metal carbonyl complexes have, in many cases, been studied by optical spectroscopy and the lowest optical transition assigned to either a triplet LC transition or a triplet MLCT transition. In some cases, the excited-state behavior for the metal carbonyl complexes is more complicated, and interpretations involving dual emitters or mixed excited-state processes have been invoked.

Excited-state processes associated with the metal center directly perturb ν(CO) in a calculable fashion. Excited-state processes that increase the electron density at the metal shift the ν(CO) band to lower energy and vice-versa for a decrease in metal electron density. Therefore, an MLCT excited state that decreases the electron density at the metal center will shift the ν(CO) band to higher energy, while a ligand-to-metal charge-transfer state or other transition that increases the metal electron density will shift the ν(CO) band to lower energy. In the case of MLCT excited states, the size of the shift is a direct measure of the degree of charge transfer (CT) in the excited state. An interesting case is the LC excited state, which neither transfers nor accepts electron density from the metal. However, in the case of a $\pi \rightarrow \pi^*$ LC excited state, the population of the antibonding orbitals is slightly electron donating relative to the ground state, which shifts ν(CO) to lower energy. Because this is a secondary effect, the shift is expected to be small. The CO ligand provides a useful tag for TRIR probing of the excited-state character and can provide information that can be used to interpret the orbital origin, metal oxidation state, and degree of back-bonding in metal carbonyl complexes. TRIR is unique in its ability to provide information for these systems by probing on a molecular scale the changes in electron density at the metal ion and the CO ligands.

1. Rhenium Dicarbonyl Complexes

A limited amount of research has appeared on rhenium dicarbonyl complexes. Turner and Ishitani have reported TRIR results on $[Re(bpy)(CO)_2\{P(OEt)_3\}_2]^+$.[50] This complex has two equivalent carbonyls related by C_{2v} symmetry, giving rise to two IR-active modes, an A_1 and a B_1 mode. Two ν(CO) bands are observed in the ground state at 1956 and 1882 cm^{-1}, which shift to 2012 cm^{-1} ($\Delta = +56$ cm^{-1}) and 1927 cm^{-1} ($\Delta = +45$ cm^{-1}) in the excited state, supporting an assignment of a lowest MLCT excited state.

2. Rhodium and Iridium Dicarbonyl Complexes

Picosecond TRIR experiments have been performed on $[Cp^*Rh(CO)_2]$, $[Cp^*Ir(CO)_2]$, and $[Ir(CO)_2(acac)]$ (where Cp* is η_5-$C_5(CH_3)_5$ and acac is acetylacetonate) in hexane to study CO photodissociation.[51]

Table 6. Time-Resolved Vibrational Data for Electronically Excited States of Transition Metal Mono- and Dicarbonyl Complexes

complex	ref(s)	study/result
$[Os(tpy)(bpy)CO]^{2+}$, $[Os(phen)_2COCl]^{+}$, $[Os(bpy)_2CO(pyridine)]^{2+}$	16	TRIR data for ν(CO) bands showing large shifts to higher energy consistent with a lowest-lying MLCT excited state following excitation
$[Re(bpy)(CO)_2\{P(OEt)_3\}_2]^{+}$	50	the ν(CO) bands showing large shifts to higher energy consistent with a lowest-lying MLCT excited state following excitation
$[Cp^*Rh(CO)_2]$, $[Cp^*Ir(CO)_2]$, $[acacIr(CO)_2]$,	51	bleach and recovery of ν(CO) bands suggesting a 40-ps excited state
[RuX(R)(CO)$_2$(L)] [X is Cl, Br, or I; R is methyl or ethyl; L is (^{i}Pr-DAB), (^{i}Pr-pyCa), or bpy]	74	TR^3 and TRIR studies of the XLCT excited state; the TR^3 experiment provides data on the degree of CT, while the TRIR experiment is a measure of metal oxidation state and percent of CT

These complexes demonstrate bleaching for the ground-state ν(CO) bands but show no signal for free CO. The bleach is recovered in ~40 ps. This behavior was attributed to relaxation of the electronic excited states, with the excited-state ν(CO) bands believed to be broadened by excess internal energy. References and overviews of time-resolved studies of transition-metal dicarbonyls are given in Table 6.

3. Rhenium Tricarbonyl Complexes

Complexes of the general form *fac*-[Re(CO)$_3$(L)X] (where L is the polypyridyl ligand and X is halide, pyridine derivative, or triphenylphosphene) and their excited states have sparked considerable interest because they can act as efficient photosensitizers and reduction catalysts for CO_2.[52,53] These complexes are ideal systems for TRIR spectroscopy studies because they have strong carbonyl bands in the 1900−2050 cm^{-1} region, relatively long-lived electronic excited states, and established synthetic chemistry.[54,55] Additionally, polypyridyl complexes of Re(I) are increasingly important in studying fundamental photochemical processes such as electron- and energy-transfer processes.[55−57] Since the initial studies of Wrighton and Morse,[52a] these complexes have continued to be important in studying the fundamental photophysics of MLCT excited states (i.e., nonradiative decay and the Marcus "inverted" region)[55d,56d,58] and the effects of different solvents and sampling media.[59] Furthermore, there is a complex interplay between MLCT and LC excited states in these systems.[59]

The *fac*-[Re(CO)$_3$(L)X] complexes possess C_s symmetry, with three IR-active modes [A′(1) + A′(2)+ A″]. Two carbonyls are trans to the L ligand, and one CO is trans to X. With L = pyridine, two ν(CO) bands are observed in the FTIR spectrum. The band at lower energy is broad, suggesting the presence of two bands close in energy, whereas with L = Cl or triphenylphosphine, three resolved CO stretches are observed.

The first TRIR measurement of the Re(I) tricarbonyl MLCT excited state was Turner's investigation of [Re(4,4′-bpy)$_2$(CO)$_3$Cl] (where 4,4′-bpy is 4,4′-bipyridine).[60] In this molecule the three observable ν(CO) bands shift to higher energy, as expected for an MLCT excited state. One band shifts +28 cm^{-1} (from 2027 to 2055 cm^{-1}), and the other two shift +66 cm^{-1} (from 1926 to 1992 cm^{-1} and from 1891 to 1957 cm^{-1}). The shifts were interpreted to arise from changes in the CO back-bonding caused by populating the bipyridyl ligand π^* states and depopulating the Re(I) dπ electronic states, consistent with partial oxidation of Re(I) to Re^{II}. This change in oxidation state decreases the Re−CO back-bonding, which increases the triple-bond character of the carbonyls.

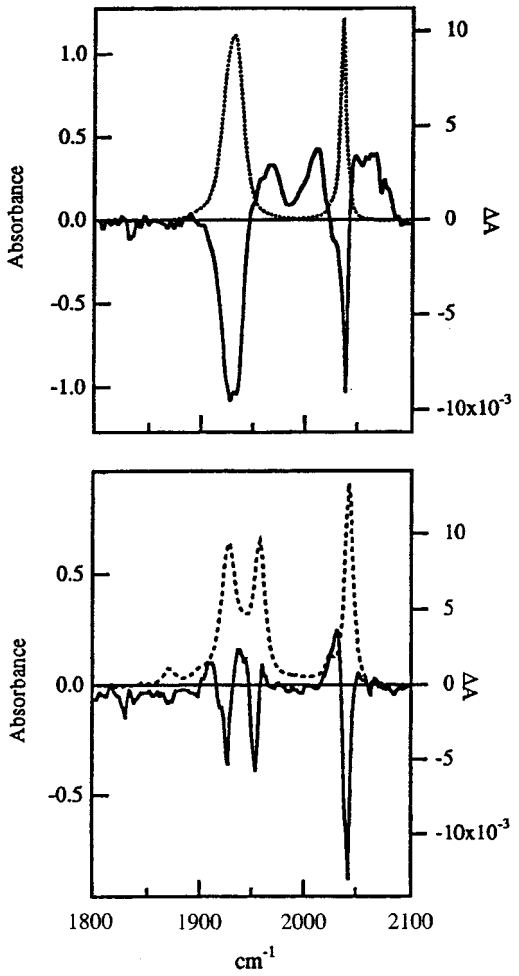

Figure 8. Ground-state (broken curve) and time-resolved difference FTIR spectra of *fac*-[Re(phen)(CO)$_3$(4-Mepy)]$^+$ (top: phen is 1,10-phenanthroline and 4-Mepy is 4-methylpyridine) and *fac*-[Re(dppz)(CO)$_3$(PPh$_3$)]$^+$ (bottom: dppz is dipyrido[3,2-*a*:2′,2′-*c*]phenazine and PPh$_3$ is triphenylphosphine) at room temperature. The transient difference spectra were measured 600 ns after 354.7-nm excitation. Sample concentrations were ~1 mM in deoxygenated CH_3CN.

The shift of CO to higher energy is a general effect for an MLCT excited state; other examples include *fac*-[Re(bpy)(CO)$_3$(4-Etpy)]$^+$ (where 4-Etpy is 4-ethylpyridine) and *fac*-[Re(bpy)(CO)$_3$Cl].[16,17,61] The TRIR and FTIR spectra for *fac*-[Re(phen)(CO)$_3$(4-Mepy)]$^+$ (where 4-Mepy is 4-methylpyridine) in the ν(CO) region are shown in Figure 8. In this spectrum, the broad ground-state ν(CO) band at 1931 cm^{-1} appears as a bleach, with new excited-state bands appearing

Table 7. Time-Resolved Vibrational Data for Electronically Excited States of Rhenium Tricarbonyl Complexes

complex	ref(s)	study/result
$[Re(4,4'\text{-bpy})_2(CO)_3Cl]$	60	first TRIR study of a $Re(CO)_3$ complex; shifts of ν(CO) to higher energy as expected for an MLCT excited state
$[Re(phen)(CO)_3(4\text{-Mepy})]^+$, $[Re(dppz)(CO)_3(PPh3)]^+$, $[Re(dppz)(CO)_3(4\text{-Etpy})]^+$, $[Re(4,4'\text{-}(NH_2)_2)bpy)(CO)_3(4\text{-Etpy})]^+$	16,17	comparison of TRIR spectra for MLCT, LC, and mixed (or dual) excited states
$[Re(bpy)(CO)_3(4\text{-Etpy})]^+$	61a,65,79	MLCT excited-state studied by TR^3 and TRIR spectroscopies
$[Re(bpy)(CO)_3Cl]$	61b	the ν(CO) bands shift to the higher energy, MLCT excited state
$[Re(benzyl)_2(CO)_3(^i\text{Pr-DAB})]$	61c	TRIR studies of the excited state from which bond homolysis occurs; state assigned to a $\sigma\pi^*$ excited state

at 1965 and 2015 cm^{-1}. The broad ground-state band is resolved into its two components because the effective symmetry of the molecule in the excited state is lower. The third ν(CO) band at 2036 cm^{-1} also shifts to higher energy (2065 cm^{-1}) in the excited state.

On the basis of optical measurements, *fac*-$[Re(dppz)(CO)_3(PPh_3)]^{+*}$ and *fac*-$[Re(dppz)(CO)_3(4\text{-Etpy})]^+$ (where dppz is dipyrido[3,2-*a*:2′,2′-c]phenazine, PPh_3 is triphenylphosphine, and 4-Etpy is 4-ethylpyridine) are classified as having LC lowest excited states (a lowest-lying, dppz-based $^3\pi\pi^*$ state).[34] As expected, the transient infrared difference spectra for these complexes show only slight shifts for the three carbonyl bands to lower energy (<5 cm^{-1}) (see Figure 8).[16,17]

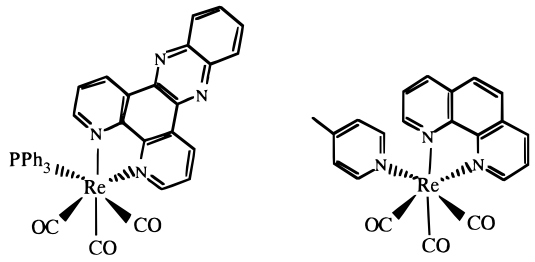

fac-$[Re(dppz)(CO)_3(PPh_3)]^+$ *fac*-$[Re(phen)(CO)_3(4\text{-Mepy})]^+$

The complex $[Re(benzyl)(CO)_3(^i\text{Pr-DAB})]$ (where ^{i}Pr-DAB is *N*,*N*′-diisopropyl-1,4-diazobutadiene) undergoes homolysis of the Re benzyl bond with excitation into the visible MLCT transition. TRIR experiments have been conducted to interrogate the intermediate excited state from which the bond homolysis occurs.[61c] The pattern of ν(CO) bands demonstrates small shifts to lower energy, and the transient is assigned to a $\sigma\pi^*$ excited state. Promoting an electron from the σ(Re benzyl) orbital to the π^*(DAB) orbital diminishes the π back-bonding in a manner similar to what occurs for the $\pi\pi^*$ excited state noted above.

An important use of TRIR spectroscopy is to resolve complex excited-state behavior in systems that have competing excited states with independent wave function descriptors (e.g., MLCT vs LC). One example of competing excited states is seen in the TRIR spectrum of *fac*-$[Re(4,4'\text{-}(NH_2)_2)\text{-bpy})(CO)_3(4\text{-Etpy})]^+$ [where 4,4′-$(NH_2)_2$)-bpy is 4,4′-diamino-2,2′-bipyridine].[16,17] The transient features observed for this complex can be explained by invoking a model of an MLCT excited-state coexisting with at least one ligand-based state ($\pi\pi^*$ or $n\pi^*$).

TRIR experiments have been the predominant probe of excited-state properties in $[Re(CO)_3(L)X]^+$ complexes (where L is bpy or 4,4′-substituted bpy). However, TR^3 spectroscopy has also been successfully applied to these systems to supply data on the polypyridyl radical anion formed after excitation.[52a,52b,63] The results are similar to the observations in ruthenium tris-polypyridine complexes. Table 7 lists the studies conducted on $Re(CO)_3$ complexes.

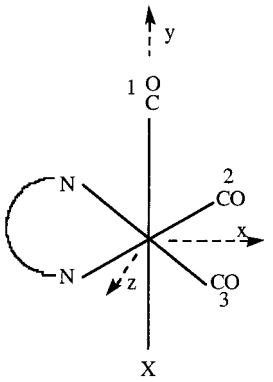

Figure 9. Coordination environment for the facial structure of a rhenium tricarbonyl complex.

4. Excited-State Analysis of Re Carbonyl Complexes

The shifts in the ν(CO) bands can be correlated to the excited-state structure in the MLCT. In the facial structure of tricarbonyl complexes, coordinates can be defined so that the *y*-axis (axial) position corresponds to the displacement vector for the stretching of CO(1) and the *x*-axis (equatorial) position passes through the middle of both the polypyridine ligand and the two displacement vectors of the stretching motions of CO(2) and CO(3) (see Figure 9). The $d_{xy} + d_{zy}$ and $d_{xy} - d_{xy}$ orbitals then have the appropriate symmetry to interact with the π^* levels of CO(1), CO(2), and CO(3), and the $d_{z^2} - d_{y^2}$ orbitals can interact with CO(2) and CO(3).

In the excited state, because carbonyls have higher π^* acceptor ability than that of the polypyridine ligand, the Re^{II} hole is localized on the $d_{z^2} - d_{y^2}$ orbital. The resulting change in π back-bonding affects the three normal modes of the carbonyls in different ways. For the Re(phen) complex, the 2062 cm^{-1} band shifts by +26 cm^{-1}, the 2011 cm^{-1} band by +80 cm^{-1}, and the 1962 cm^{-1} band by +31 cm^{-1}. These shifts support the idea of a localized hole in the $d\pi$ orbital configuration in the excited state. Additionally, in the MLCT state of these complexes, significant differences exist in the sizes of the shifts in the carbonyl bands with different polypyridyl ligands (see Table 8).[63] These different shifts can be attributed to differences in the extent of charge

Table 8. Comparison of ν(CO) Bands (cm^{-1}) Following MLCT Excitation for Different [$Re^{I}(CO)_3$(polypyridyl)] Complexes

complex	ground state	excited state	Δ
$[Re(phen)(CO)_3(4\text{-}Mepy)]^+$	2036, 1931	2062, 2011, 1962	26, 80, 31
$[Re(4,4'\text{-}bpy)_2(CO)_3Cl]$	2027, 1926, 1891	2055, 1992, 1957	28, 66, 66
$[Re(4,4'\text{-}(CH_3)_2bpy)(CO)_3(4\text{-}Etpy)]^+$	2034, 1927	2067, 2008, 1964	33, 81, 37
$[Re(4,4'\text{-}(CH_3O)_2bpy)(CO)_3(4\text{-}Etpy)]^+$	2033, 1921	2070, 2008, 1962	34, 87, 41
$[Re(bpy)(CO)_3(4\text{-}Etpy)]^+$	2035, 1927	2074, 2010, 1971	39, 83, 44
$[Re(4,4'\text{-}(CO_2Et)_2bpy)(CO)_3(4\text{-}Etpy)]^+$	2038, 1935	2092, 2023, 1976	41, 88, 54

Table 9. Time-Resolved Vibrational Studies for Electronically Excited States of Transition Metal Tetracarbonyl Complexes

complex	ref(s)	study/result
$[Re(CO)_4(phen)]^+$	16	in TRIR spectra, the ν(CO) bands shift slightly to higher energy consistent with a LC excited state with some CT character
$[W(CO)_4L]$; L is bpy, dmb, or pyridine-2-carbaldehyde isopropylimine	66	the TR^3 data show Raman shifts consistent with the MLCT excited state; the ν(CO) band shifts by +50 cm^{-1}

transfer to the bipyridine ligand in the MLCT state, which in turn affect the degree of π back-bonding (see Table 8). Because of substantial coupling between carbonyl groups, the variable to compare is not the CO frequency but the CO force constant. Turner has applied a more quantitative description of the excited-state effects on the carbonyls by using an energy-factored force-field (EFFF) estimate.[64] This approximation takes into account the principal force constants in the CO bond and the interaction force constants between the different carbonyls. By comparing the shifts, the change in CO bond length in the excited state can be related to the EFFF force constant by this expression:

$$r_{CO} = (1.647 - 0.184)\ln(k_{CO}) \qquad (5)$$

where r is in angstrom and k is in millidyne per angstrom. In principle, k_{CO} can be related to the degree of charge transfer. The CO displacements in the excited-state calculated with eq 5 are small, on the order of −0.01(0) Å. Changes in the CO bond length track the qualitative description above. As predicted, the calculated shifts for the non-MLCT excited states are significantly smaller.

5. Rhenium Tetracarbonyl Complexes

The class of Re(I) carbonyl complexes of the type $[Re(CO)_4(L)]$ (where L is bpy or phen) exhibit unique excited-state behavior; the best description of the excited state obtained with electronic spectroscopy is nominally LC with an admixture of 1−3% charge-transfer character.[65,66] The tetracarbonyl systems have C_{2v} symmetry, with the C_2 axis defined so that it intersects the Re center and the 2,2′-C−C bond of the bipyridyl ligand. Consequently, there are four IR-active carbonyl modes for these molecules: (1) an A_1 mode, which is a linear combination of the in-phase motion of the trans carbonyls, (2) the analogous A_1 mode involving the cis carbonyls, (3) a B_1 mode for the out-of-phase motion of the cis carbonyls, and (4) the analogous B_2 mode arising from the trans carbonyls.

In the first reported TRIR spectrum of a rhenium tetracarbonyl complex, the three observed ν(CO) bands showed shifts of about +6 cm^{-1} in the excited state.[16] The positive shifts seen were not predicted for an LC state and were interpreted as showing the effect of charge-transfer character on the nominal LC excited state.

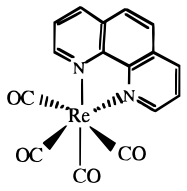

$[Re(CO)_4(phen)]^+$

6. Tungsten Tetracarbonyl Complexes

TR^3 experiments have been conducted on $[W(CO)_4(L)]$ complexes (where L is bpy, dmb, or pyridine-2-carbaldehyde isopropylimine).[67] Spectra were measured of the lowest MLCT state in CH_3CN following 406-nm excitation. The excited-state bands were attributed to ring deformation modes of the L ligand. The Raman shifts for the bpy and dmb bands were similar to those observed in Ru and Re MLCT states, and the ν_s(CO) band shifted by +50 cm^{-1}. Studies conducted on tetracarbonyl complexes are listed in Table 9.

7. Tungsten Pentacarbonyl Complexes

For $[W(CO)_5]L$ (where L is pyridine, 4-substituted pyridine, or piperidine), the competing LF and MLCT states can be directly probed by TRIR spectroscopy. In $[W(CO)_5(4\text{-}Acpy)]$ and $[W(CO)_5(4\text{-}CNpy)]$, the equilibrium between the higher-lying LF (∼4000 cm^{-1}) and the lowest-lying charge-transfer excited state was studied.[68] These complexes possess C_{4v} ground-state symmetry, giving rise to two bands for a_1 modes (∼2072 and 1925−1930 cm^{-1}) and a band for an e mode (∼1936 cm^{-1}). Initial excitation into the lowest MLCT state shifts the ν(CO) bands to higher energy (for $[W(CO)_5(4\text{-}Acpy)]$, Δ is +41 cm^{-1} for the a_1 mode and +64 cm^{-1} for the e mode; for $[W(CO)_5(4\text{-}CNpy)]$, Δ is +36 cm^{-1} for the a_1 mode and +64 cm^{-1} for the e mode). The experimental apparatus could not measure the band for the remaining a_1 mode. Loss of the excited-state spectrum after 2.5 μs and observation of a new band in both complexes at 1957 cm^{-1} were consistent with the population of the LF state

Table 10. Time-Resolved Vibrational Data for Electronically Excited States of Transition Metal Pentacarbonyl Complexes

complex	ref(s)	study/result
$[W(CO)_5(4\text{-Acpy})]$, $[W(CO)_5(4\text{-CNpy})]$, $[W(CO)_5(4,4'\text{-bpy})]$	67,68	the TRIR data showing an initial MLCT excited state at early times which decays to an LF excited state and decomposition to a $W(CO)_5$ solvent species
$[W(CO)_5L]$; L is pyridine or piperidine	69	the TRIR data consistent with an LF excited state with CO bond lengths studied by EFFF analysis
$[(CO)_5W(4,4'\text{-bpy})W(CO)_5]$, $[(CO)_5W(\text{pyrazine})W(CO)_5]$	71,72	TR^3 and TRIR studies consistent with MLCT excited state with a mixed-valence oxidation state description
$[(CO)_5W(OR)R']$; (R and R′ are CH_3, R is CH_3 and R′ is *p*-tolyl, or R is ethyl and R′ is phenyl)	73	photoinduced isomerization studied by TR^3 spectroscopy

and decomposition to the $W(CO)_5$-solvent species, suggesting that the LF and charge-transfer states are in equilibrium at room temperature. Similar results were obtained for $[W(CO)_5(4,4'\text{-bpy})]$.[63]

TRIR data was used to interpret the excited-state structure of $[W(CO)_5L]$ (where L is pyridine or piperidine) using EFFF analysis.[69] In these complexes, the lowest excited state is characterized as an LF ($^1A_1 \rightarrow {}^3E$) state, and a time-dependent preresonant Raman analysis predicts that the CO bond lengths will decrease in the excited state relative to the ground state.[70] The spectra exhibited shifts to lower energy corresponding to an unexpected lengthening for the carbonyls in the LF state, with the three ν(CO) bands shifting by -129, -43, and -118 cm^{-1} (for L = pyridine). EFFF analysis shows that the carbonyl bonds lengthen, with the changes in bond length for equatorial carbonyls being larger than for the axial carbonyls, and that the angle between CO_{eq} and the CO_{ax} increases.

TRIR has also been used to study the electron distribution and excited-state properties of tungsten carbonyl dimers of the type $[(CO)_5W(L)W(CO)_5]$ (where L is 4,4′-bpy or pyrazine).[71] Initial excitation into the MLCT excited state produces a mixed-valence excited state. TRIR studies show that the excited state is localized on one-half of the dimer, with small electronic coupling. A recent TR^3 study of $[(CO)_5W(4,4'\text{-bpy})W(CO)_5]$ has suggested that the same excited-state description applies for this complex.[72] The shifts of the ν(CO) bands in the TRIR study directly measure the electron density on the metal (oxidation state). In the TR^3 spectrum the ν(CO) band at 2070 cm^{-1} is depleted, with a concomitant growth of bipyridyl radical anion bands at 1350 and 1510 cm^{-1}. No new Raman bands were observed in the carbonyl region.

8. Tungsten Carbyne Complexes

Transient vibrational studies can provide insight into the photophysics of other organometallic species. For example, TR^3 experiments have been used to study the excited-state properties of tungsten carbyne complexes.[73] Complexes of the type $[(CO)_5W(OR)R']$ [where R and R′ are CH_3 (**1**) or R is CH_3 and R′ is *p*-tolyl (**2**) or R is ethyl and R′ is phenyl (**3**)] exhibit photoinduced anti- and syn-conformer isomerization. For complex **1** the TR^3 data showed only small changes. However, in complexes **2** and **3** the 1235 cm^{-1} band shifts by $+35$ cm^{-1}, which was attributed to the isomerization of the anti conformer to the syn conformer. The lack of large shifts in complex **1** arises from a reversible anti-syn isomerization in the alkyl complex caused by the lack of steric restrictions. Excited-state studies of pentacarbonyl complexes are listed in Table 10.

9. Ruthenium and Osmium Carbonyl Complexes

Both TR^3 and TRIR spectroscopy have been used to interpret the excited-state character of $[RuX(R)(CO)_2(L)]$ [where X is Cl, Br, or I; R is methyl or ethyl; and L is *N*,*N*′-diisopropyl-1,4-diaza-1,3-butadiene (^{i}Pr-DAB); pyridine-2-carbaldehyde-*N*-isopropylamine (^{i}Pr-pyCa), or bpy].[74] These complexes are unique in that their lowest excited state is best described as a mixture of MLCT and XLCT (halide-to-ligand charge-transfer) character. The shifts of the ν(CN) and ν(CO) bands directly measure the percentage of XLCT character, which increases when X is changed successively from Cl to Br to I.

For $[RuCl(Me)(CO)_2(^i\text{Pr-DAB})]$, the ν(CN) band at 1490 cm^{-1} shifts by -70 cm^{-1}, and ν(CO) shifts from 2035 to 1940 cm^{-1} ($\Delta = -95$ cm^{-1}). By comparison, the shift of the ν(CN) band in the iodide complex is much larger, corresponding to an increase in the charge transferred to the ligand. Similar trends were observed for the other complexes. The TR^3 experiment provides data on the degree of charge transfer, while the shifts for the ν(CN) and ν(CO) bands in the TRIR experiment directly measure the metal oxidation state and the percentage of XLCT in the charge-transfer state. It was concluded that the shifts correspond to a change in the type of charge transfer to the L ligand arising from changes in the percentage of XLCT in the excited state.

Significant positive shifts in the carbonyl bands of Os(II) complexes containing CO ligands indicate the presence of MLCT excited states. The transient difference spectrum of $[Os(tpy)(bpy)CO]^{2+}$ (where tpy is 2,2′:6′,2″-terpyridine) in CH_3CN measured with the step-scan technique shows a shift of $+70$ cm^{-1} of the CO band, from 1974 to 2044 cm^{-1}. This data compares to shifts of $+73$ cm^{-1} for $[Os(phen)_2COCl]^+$ and $+69$ cm^{-1} for $[Os(bpy)_2CO(pyridine)]^{2+}$.[16] The data for mono- and dicarbonyl complexes is compared in Table 6.

V. Molecular Assemblies

Following electronic excitation, inorganic complexes in solution can undergo energy or electron transfer. Charge separation following absorption of a photon and the ability to convert optical energy are important components of natural photosynthesis. For

Scheme 2[a]

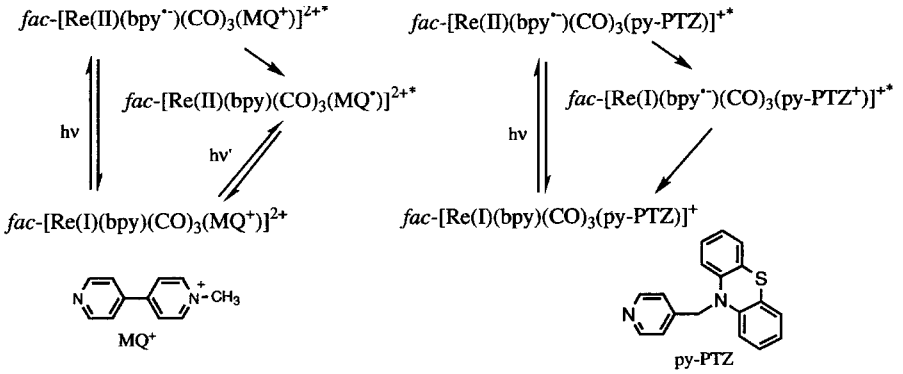

[a] In CH_3CN at 298 K.

inorganic complexes, most charge-separation systems involve intermolecular electron transfer, but intramolecular electron transfer has also been observed.[75] To continue to develop and control energy conversion processes, a substantial understanding of photophysical properties of these chromophore−quencher assemblies is required. This understanding includes knowledge of the electronic and molecular structures of excited states and the intermediates formed after excitation.

Recently, inorganic photochemistry has focused on studying more complex or supramolecular assemblies.[76] These polynuclear coordination compounds are typically large molecules with two or more transition-metal complex subunits linked by a suitable bridging ligand. Because of their more complex molecular architecture, the photochemistry and photophysics of these systems are usually more complicated. Therefore, the study of intracomponent and intercomponent processes represents a considerable challenge in which time-resolved vibrational spectroscopies have begun to play a significant role.

A. Intramolecular Chromophore–Quencher Complexes

TR^3 measurements have been used to identify the electron-transfer products that appear upon photolysis of a mixture of donors and acceptors in solution.[77] The first TR^3 experiment on an intramolecular system studied excited-state electron transfer in a covalently linked porphyrin viologen complex.[78] Meyer and co-workers have applied TR^3 spectroscopy to a series of inorganic systems undergoing intramolecular electron transfer.[69,79] These systems have included chromophore−quencher complexes based on $Re(CO)_3(bpy)$, Re dimers, and modified amino acid assemblies. Transient absorption and emission spectroscopies have been the methods of choice for studying light-induced electron transfer in chromophore−quencher complexes, but transient vibrational techniques can greatly complement these studies by identifying intermediates and determining their detailed structures. Changes in structure and conformation induced by electron transfer can be inferred from changes in the vibrational band energies and the relative intensities of the Raman or IR bands.

Two examples of chromophore−quencher complexes are *fac*-$[Re(bpy)(CO)_3(MQ^+)]^{2+}$ (where MQ^+ is *N*-methyl-4,4′-bipyridinium cation or monoquat) and *fac*-$[Re(bpy)(CO)_3(py\text{-}PTZ)]^+$ [where py-PTZ is 10-picol-4-ylphenothiazine]. These two complexes undergo oxidative or reductive quenching following $d\pi[Re^{II}] \rightarrow \pi^*(bpy)$ excitation (see Scheme 2).

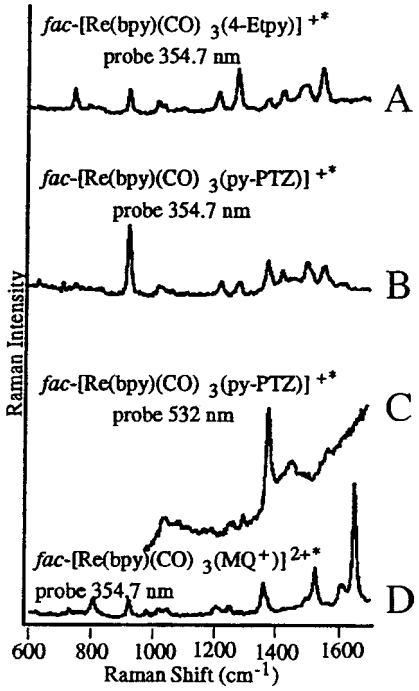

Figure 10. Transient resonance Raman spectra from 600 to 1700 cm^{-1} for (A) *fac*-$[Re(bpy)(CO)_3(4\text{-}Etpy)]^+$ (354.7-nm pulse/probe), (B) *fac*-$[Re(bpy)(CO)_3(py\text{-}PTZ)]^+$ (354.7-nm pulse/probe), (C) *fac*-$[Re(bpy)(CO)_3(py\text{-}PTZ)]^+$ (354.7-nm pulse/ 532-nm probe), and (D) *fac*-$[Re(bpy)(CO)_3(MQ^+)]^{2+}$ (354.7-nm pulse/probe). All sample concentrations were ~1 mM in CH_3CN and freeze/pump/thaw degassed at least three cycles before being sealed under vacuum.

Comparing the TR^3 spectra of *fac*-$[Re(bpy)(CO)_3(4\text{-}Etpy)]^{+*}$ and *fac*-$[Re(bpy)(CO)_3(MQ^+)]^{2+*}$ (Figure 10, CH_3CN, 298 K, 354.7-nm excitation, 354.7-nm probe) shows an absence of $bpy^{\bullet-}$-based bands in the MQ^+ complex, indicating that $bpy^{\bullet-} \rightarrow$ -MQ^+ electron transfer occurs. For *fac*-$[Re(bpy)(CO)_3(MQ^+)]^{2+*}$, only bands originating from -$MQ^{\bullet}$ are seen in the transient spectrum, while in contrast the resonantly enhanced Raman bands for *fac*-$[Re(bpy)(CO)_3(4\text{-}Etpy)]^{+*}$ are typical of $bpy^{\bullet-}$.[65,79]

Information about the transient structural changes at -MQ^+ that accompany intramolecular electron

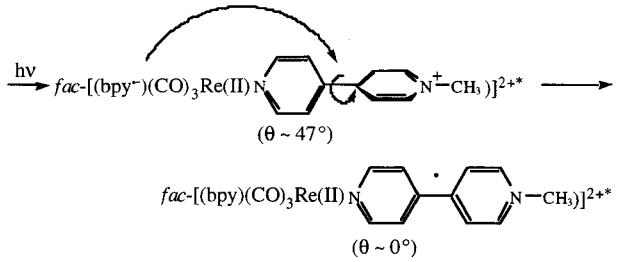

Figure 11. Excited-state structural changes of *fac*-[Re(bpy)(CO)$_3$(MQ$^+$)]$^{2+}$ following absorption of a photon.

transfer have been inferred from the Raman data.[79] The data demonstrate an increase in the inter-ring −C−C− bond order and a decrease in the inter-ring separation distance, both of which are consistent with a planar, quinoidal structure in the excited state, with the angle θ between pyridyl planes near 0°. From X-ray crystallography, θ is 47°. In the ground state of *fac*-[Re(bpy)(CO)$_3$(MQ$^+$)]$^{2+}$, this angle represents a balance between H−H repulsion between the linked rings, which is minimized at θ = 90°, and electronic delocalization, which is maximized at θ = 0°. Upon electron transfer to MQ$^+$, θ decreases to 0° (see Figure 11). The energy difference between $\theta \approx$ 47° and $\theta \approx$ 0° for *fac*-[Re(bpy)(CO)$_3$(MQ$^{\cdot}$)]$^{2+}$* is ~0.3 eV, with the $\theta \approx$ 0° form favored in the transient species because of enhanced delocalization energy.

Figure 10 compares the TR^3 spectra of *fac*-[Re(bpy)(CO)$_3$(4-Etpy)]$^{+}$* (354.7-nm pulse/probe), *fac*-[Re(bpy)(CO)$_3$(py-PTZ)]$^{+}$* (354.7-nm pulse/probe), and *fac*-[Re(bpy)(CO)$_3$(py-PTZ)]$^{+}$* (354.7-nm pulse/532-nm probe). Following Re^{I}(dπ) → bpy(π*) in CH$_3$CN, the spectra of *fac*-[Re(bpy)(CO)$_3$(py-PTZ)]$^{+}$* contain the expected features for bpy$^{\cdot-}$. That electron transfer from -PTZ to Re^{II} occurs is made clear by the appearance of resonantly enhanced -PTZ$^{\cdot+}$ bands using 532-nm laser pulses (this wavelength is within a region of $\pi \rightarrow \pi$* absorption for -PTZ$^{\cdot+}$).

In molecular assemblies containing both covalently attached donors and acceptors, excitation followed by electron transfer can lead to intramolecular redox separation. The advantage of using metal complexes in these assemblies is that coordination chemistry creates molecular spacers between the donor and acceptor with ligand bridges. TR^3 measurements of [(py-PTZ)(CO)$_3$Re(μ-bbpe)Re(CO)$_3$(MQ$^+$](PF$_6$)$_3$ in CH$_3$CN demonstrate that following simultaneous Re^{I}(dπ)→bbpe(π*) and $\pi\rightarrow\pi$*(bbpe) excitation a series of intramolecular electron-transfer events leads to the redox-separated state [(py-PTZ$^{\cdot+}$)(CO)$_3$Re^{I}(μ-bbpe)Re^{I}(CO)$_3$(MQ$^{\cdot}$)]$^{3+}$.[80]

The same experimental approach was used to study electron transfer in molecular assemblies based on amino acids.[81] The complex Anq-Lys(Ru^{II}(bpy)$_2$m)-PTZ]$^{2+}$ (where Anq is anthraquinone, Lys is the derivatized lysine, and m is 4′-methyl-2,2′-bipyridyl-4′-carbonyl) was studied following Ru(II) → polypyridyl MLCT excitation. The transient resonance Raman spectrum (354.7-nm excitation/354.7-nm probe) of [Ru(bpy)$_2$(m-NHCH$_3$)]$^{2+}$ (where m-NHCH$_3$ is 4′-methyl-2,2′-bipyridyl-4′-methyl amide) established that the excited electron is primarily localized at the π* level of the m-NHCH$_3$ ligand in the equilibrated excited state. No bands for m-NHCH$_3^{\cdot-}$ or bpy$^{\cdot-}$ were observed in the spectrum of the assembly under identical conditions, but excitation at 354.7 nm and probing at 532 nm caused resonantly enhanced bands characteristic of -PTZ$^{\cdot+}$ and -Anq$^{\cdot-}$ to appear.[81] Vibrational spectroscopy studies of intramolecular chromophore−quencher complexes are listed in Table 11.

B. Polypyridyl-Bridged Dimers

Ligand-bridged metal complexes have provided a way to study intramolecular processes from both theoretical and experimental standpoints.[82,83] The bridging ligand has been shown to be an important parameter that can control the physical properties of these systems. The goal has been to understand light-induced energy and electron-transfer processes in these linked systems for potential applications in photochemically driven molecular devices.

The bridging ligand can provide control over intercomponent processes, serving not only as a structural link but also as a way to modulate electron- or energy-transfer rates. The complex [(bpy)$_2$Ru^{II}-ABRe^{I}(CO)$_3$Cl]$^{2+}$ (where AB is 2,2′:3′2″:6″,2‴-quaterpyridine) is an example where an asymmetric bridge (AB) contains two inequivalent metal binding sites, one more sterically hindered than the other.[84] The difference between the A and B sites is expected to perturb the MLCT energy level of the attached Re(I) or Ru(II) chromophores, thereby controlling the direction of energy transfer in the ReABRu and RuABRe isomers.

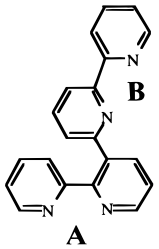

The excited state of [(bpy)$_2$Ru^{II}ABRe^{I}(CO)$_3$Cl]$^{2+}$ in CH$_3$CN has been characterized by step-scan TRIR spectroscopy.[16] The ν(CO) bands shift to slightly lower energy following excitation. The band at 2023 cm^{-1} shifts to 2016, the band at 1918 cm^{-1} shifts to 1910 cm^{-1}, and the band at 1902 cm^{-1} shifts to 1888 cm^{-1}. The magnitudes and directions of these shifts

Table 11. Time-Resolved Vibrational Data for Intermediates Formed Following Electronic Excitation of Intramolecular Chromophore−Quencher Complexes Based on d^6 Transition Metals

complex	ref(s)	study/result
[Re(bpy)(CO)$_3$(MQ$^+$)]$^{2+}$, [Re(bpy)(CO)$_3$(py-PTZ)]$^+$	65,79	TR^3 studies providing structural insights into the transient species which exists following MLCT excitation and intramolecular electron transfer
[(py-PTZ)(CO)$_3$Re(μ-bbpe)Re(CO)$_3$(MQ$^+$)]$^{3+}$, [Anq-Lys(Ru(bpy)$_2$m-)(py-PTZ]$^{2+}$	80,81	the TR^3 data showing excited-state structure following MLCT excitation followed by a series of electron-transfer events

Table 12. Time-Resolved Vibrational Data for Electronically Excited States of Polypyridyl-Bridged Dinuclear Complexes

complex	ref(s)	study/result
$[(bpy)_2RuABRe(CO)_3Cl]^{2+}$, $[(bpy)_2RuBARe(CO)_3Cl]^{2+}$	16	the ν(CO) shifts providing excited-state structural information in terms of which metals are oxidized in the excited states of the different isomers
$[(bpy)_2Ru(bpt)Ru(phen)_2]^{3+}$, $[(phen)_2Ru(bpt)Ru(bpy)_2]^{3+}$	85	TR^3 data demonstrating localization of the excited state on the Ru(bpy) unit regardless of the coordination environment of the bpt bridge
$[(Me_2phen)_2Ru(Mebpy\text{-}CH_2\text{-}CH_2\text{-}Mebpy)Rh(dmb)_3]^{5+}$	86	TR^3 studies of the complex and relevant mononuclear models assisting in determining the intercomponent processes which occur following excitation

suggest that, following initial excitation into MLCT transitions centered on the Re or the Ru, energy transfer occurs to give a $Ru^{III}-AB^{\cdot-}$ MLCT state, $[(bpy)_2Ru^{III}(AB^{\cdot-})Re^{I}(CO)_3Cl]^{2+}$*. The reduced AB bridge effectively increases the electron density on the Re, causing an increase in π back-bonding and a decrease in the CO stretching frequencies. In the ReABRu isomer, the TRIR data suggest the presence of both a $Re^{II}-AB^{\cdot-}$ and a $Ru^{III}AB^{\cdot-}$ MLCT excited state at room temperature.

TR^3 spectra have been measured for two mixed-ligand complexes, $[(bpy)_2Ru(bpt)Ru(phen)_2]^{3+}$ and $[(phen)_2Ru(bpt)Ru(bpy)_2]^{3+}$ (where bpt is 3,5-bis-(pyridin-2-yl)-1,2,4-triazole) in acetone/water solution. The two nitrogen atoms of the triazole ring possess different σ-donor properties and are therefore not equivalent. The TR^3 spectra of both complexes correspond to the spectrum of $[Ru(bpy)_3]^{3+}$*, suggesting that excitation is localized on the bpy-coordinated Ru center as $Ru^{III}(bpy^{\cdot-})$, irrespective of the coordination environment of the bpt^- ligand.[85] In a similar experiment, TR^3 spectra were compared for $[Ru(dmb)_3]^{2+}$*, $[Ru(Me_2phen)_3]^{2+}$*, and $[Ru(Me_2phen)_2(Mebpy\text{-}CH_2-CH_2\text{-}Mebpy)]^{2+}$* (where Me_2phen is 4,7-dimethyl-1,10-phenanthroline and Mebpy is 4-methyl-2,2′-bipyridine) to assist in unraveling the four intercomponent processes that occur in $[(Me_2phen)_2Ru^{II}(Mebpy\text{-}CH_2\text{-}CH_2\text{-}Mebpy)Rh^{III}(dmb)_3]^{5+}$.[86] Table 12 lists the various studies conducted on polypyridyl-bridged systems.

C. Cyano-Bridged Oligomers

The cyano bridge is a common structural motif in supramolecular complexes. Transient and CW emission studies on polynuclear complexes based on cyano-bridged $Ru(bpy)_2^{2+}$ units have revealed that intramolecular energy transfer can be controlled between the C- and N-bonded units by the linkage (see Scheme 3). There is relatively strong electronic coupling between the metal centers across the cyano bridge, and intramolecular energy transfer can occur from C-bonded to N-bonded units with unit efficiency. This chemistry has led to the design of a molecular assembly that can sensitize semiconductors in the visible[87] and to oligomers that can act as molecular conduits for long-range energy transfer.[88]

Directional energy transfer has been demonstrated in the TR^3 spectra of $[(NC)(phen)_2Ru(CN)Ru(bpy)_2(CN)]^+$ and $[(NC)(bpy)_2Ru(CN)Ru(phen)_2(CN)]^+$.[89] In this pair, the exchange of phen for bpy is nearly isomorphous electronically because the lowest-lying π* acceptor levels have comparable energies. The two ligands can be distinguished unambiguously by the fingerprinting of their Raman spectra. The transient spectrum of $[(NC)(phen)_2Ru(CN)Ru(bpy)_2(CN)]^+$* shows enhancement only of the $bpy^{\cdot-}$ bands, which is consistent with facile, cross-bridge energy transfer. In confirmation of this result, only enhanced $phen^{\cdot-}$ bands are seen in transient measurements of $[(NC)(bpy)_2Ru(CN)Ru(phen)_2(CN)]^+$*. TRIR studies of this complex are also consistent with energy transfer to the N-bonded chromophore.[16]

In the polynuclear complex $[(NC)(bpy)_2Ru(CN)Ru(4,4'\text{-}(CO_2H)_2bpy)_2(NC)Ru(bpy)_2(CN)]^{2+}$ [where 4,4′-$(CO_2H)_2$bpy is 4,4′-$(CO_2H)_2$-2,2′-bipyridine], the two carboxylic acid groups of the central Ru bridge provide binding sites on the surface of TiO_2 semiconductor electrodes. Excitation of either $Ru(bpy)_2$ unit is followed by rapid energy transfer to the central Ru to give the lowest-energy MLCT excited state. TR^3 studies on $[(NC)(bpy)_2Ru(CN)Ru(dcb)_2(NC)Ru(bpy)_2(CN)]^{2-}$* support the conclusion that energy transfer to the center occurs.[87] The spectrum lacks the typical intense $bpy^{\cdot-}$ bands, and Raman bands appear that are also seen in the TR^3 spectra of $[Ru(dcb)_2(CN)_2]^{4-}$* and $[Ru(4,4'\text{-}(CO_2H)_2bpy)_3]^{2+}$*.

The complex $[(phen)(CO)_3Re(NC)Ru(bpy)_2(CN)]^+$ is an example of a polynuclear complex designed to produce vectorial energy transport. Energy transfer is expected from the higher-energy Re-based MLCT state to the Ru-based MLCT state.[61] TR^3 studies on the nanosecond time scale reveal that rapid $Re^{II}(phen^{\cdot-}) \rightarrow Ru^{II}(bpy)$ energy transfer occurs following $Re(I) \rightarrow$ phen excitation. TRIR measurements support this conclusion (see Figure 12). In the infrared spectrum of the ground state of CH_3CN, ν(CO) bands

Scheme 3[a]

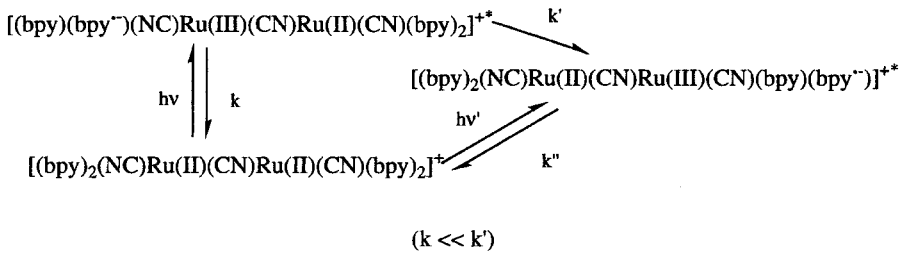

[a] In CH_3CN at 298 K.

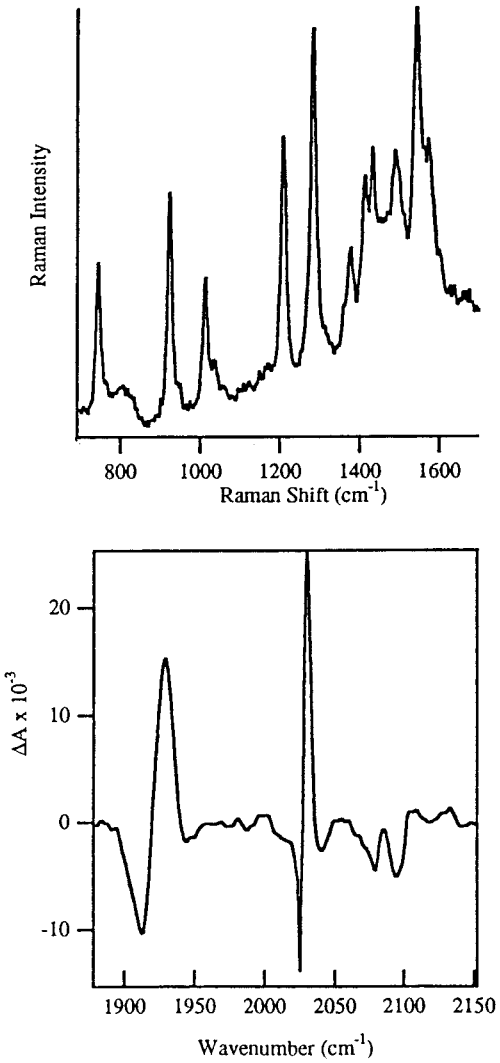

Figure 12. TR^3 spectrum (top: 700−1700 cm^{-1}) and TRIR spectrum (bottom; 1850−2150 cm^{-1}) of $[(phen)(CO)_3Re(NC)Ru(bpy)_2(CN)]^+$ in CH_3CN at room temperature.

appear at 1920 and 2028 cm^{-1}, there is a terminal ν(CN) stretch at 2081 cm^{-1}, and a ν(CN) band appears for the bridge at 2100 cm^{-1}. Spectra obtained 400 ns after 354.7-nm excitation show that the terminal ν(CN) stretch shifted from 2081 to 2108 cm^{-1}. The shifts in ν(CO) are small [$\Delta\nu$(CO) ≈ 5 cm^{-1}] compared to the large shifts for $Re^{II}(bpy^{\cdot-})$ MLCT states. These observations are consistent with the oxidation-state distribution of Re^I and Ru^{III} in the transient nanosecond lifetime intermediate. These observations also demonstrate that rapid $Re^{II}(phen^{\cdot-})$ → Ru^{II}(bpy) energy transfer occurs following Re^I → phen excitation.

Picosecond TRIR measurements show the presence of the initial $Re^{II}(phen^{\cdot-})$ state.[61] Time features seen ~1 ps after laser-flash excitation at 300 nm resemble those of an MLCT state, with ground-state bleaches near 1930 and 2030 cm^{-1} and large positive shifts in ν(CO). These features decay in 5 ps. The transient spectrum after 40 ps is similar to the spectrum observed in the nanosecond study, suggesting that after ~40 ps, $[(phen)(CO)_3Re^I(NC)Ru^{III}(bpy^{\cdot-})(bpy)(CN)]^{+*}$ is fully formed.

Cyano-bridging chemistry has been extended to the oligomers $[(phen)(CO)_3Re(CN)[Ru(bpy)_2(CN)]_nRu(bpy)_2]^{(n+1)+}$ (where $n = 0-3$). In this series, each Ru(II) unit is bridged by two cyanides (with one carbon and one nitrogen bond for each Ru). TR^3 measurements have been used to obtain direct evidence for directional energy transfer to the terminal unit.[88] Spectra for $[(phen)(CO)_3Re(NC)Ru(bpy)_2(CN)]^{+*}$, $[(phen)(CO)_3Re(NC)Ru(phen)_2(CN)]^{+*}$, and $[(phen)(CO)_3Re(NC)Ru(phen)_2(CN)Ru(bpy)_2(CN)]^{2+*}$ in CH_3CN were compared. Simultaneous Re(I) → phen, Ru(II) → phen/bpy excitation of $[(phen)(CO)_3Re(NC)Ru(phen)_2(CN)Ru(bpy)_2(CN)]^{2+}$ produces only $bpy^{\cdot-}$ bands, consistent with complete energy transfer to the terminal Ru during the laser pulse (which lasts ~10 ns).

Picosecond TRIR spectroscopy has also been used to study photoinitiated electron transfer in the cyano-bridged mixed-valence dimer $[(NC)_5Ru^{II}(CN)Ru^{III}(NH_3)_5]^-$ (see Scheme 4).[90]

Scheme 4

$$[(NC)_5Ru(II)(CN)Ru(III)(NH_3)_5]^- \underset{k_{et}}{\overset{h\nu}{\rightleftharpoons}} [(NC)_5Ru(III)(CN)Ru(II)(NH_3)_5]^-$$

Excitation into the metal−metal charge-transfer band reduces the Ru amine site, which undergoes back-electron transfer with a time constant of 6 ps, as monitored by $\nu_{terminal}$(CN). A new IR absorption band at 2110 cm^{-1} assigned to the charge-transfer excited state decayed within 0.5 ps, suggesting that back electron transfer occurs on the femtosecond time scale. Other transient features are consistent with vibrational cooling of the vibrationally hot ground-state molecule formed after back electron transfer. The data demonstrate that the rate constant for vibrational relaxation increases with increasing vibrational quantum number and that a large amount of energy, upon back-electron transfer, is placed in a single vibrational mode—the terminal CN stretch. The studies conducted on cyano-bridged oligomers are presented in Table 13.

Table 13. Time-Resolved Vibrational Data for Electronically Excited States of Cyano-Bridged Oligomers

complex	ref(s)	study/result
$[(NC)(phen)_2Ru(CN)Ru(bpy)_2(CN)]^+$, $[(NC)(bpy)_2Ru(CN)Ru(phen)_2(CN)]^+$	16,89	TR^3 and TRIR studies demonstrating energy transfer following MLCT excitation to the N-bonded chromophore
$[(NC)(bpy)_2Ru(CN)Ru(4,4'-(CO_2H)_2bpy)_2(NC)Ru(bpy)_2(CN)]^{2+}$	87	TR^3 data suggesting an antenna effect following excitation with energy transfer to the central Ru unit
$[(phen)(CO)_3Re(NC)Ru(bpy)_2(CN)]^+$, $[(phen)(CO)_3Re(CN)[Ru(bpy)_2(CN)]_nRu(bpy)_2]^{(n+1)+}$, $(n = 0-3)$	61a,96	energy transfer processes following excitation studied with TRIR and TR^3 spectroscopies, demonstrating directional energy transfer to the terminal N-bonded Ru unit
$[(NC)_5Ru^{II}(CN)Ru^{III}(NH_3)_5]^-$	90	picosecond TRIR studies of back electron transfer

D. Zeolite-Entrapped Ruthenium Complexes

One of the goals in the molecular assembly of photonic devices is to incorporate molecular components in an organized manner that facilitates a net chemical conversion. TR^3 spectroscopy has been used to study the excited states and electron-transfer processes following excitation of Ru^{II}−polypyridine complexes incorporated into Y-type zeolite matrixes.

The TR^3 spectrum of $[Ru(bpy)_3]^{2+*}$ in zeolite Y supercages has been measured and has indicated that encapsulation has only a minimal effect on the excited-state structure.[91,92] Additionally, several homoleptic and heteroleptic polypyridine complexes of Ru(II) have been studied and their TR^3 spectra in zeolite supercages compared to their spectra in aqueous solution.[93] The spectra showed ligand localization in solution and only minor spectral differences, suggesting that entrapment introduced no major structural modifications or changes in electronic distribution.

Photoinduced electron transfer has been demonstrated between $[Ru(bpy)_3]^{2+}$ and acceptors in zeolite cages. Dutta and co-workers have encapsulated $[Ru(bpy)_3]^{2+}$ and methyl viologen within zeolite cages and have studied electron transfer using transient emission and TR^3 spectroscopy.[94] After 354.7-nm excitation the TR^3 spectrum showed Raman bands produced by both $[Ru(bpy)_3]^{2+*}$ and the methyl viologen radical cation on the nanosecond time scale. These studies demonstrate the value of TR^3 spectroscopy for studying the photophysics of assemblies made from adsorption or entrapment of inorganic complexes.

VI. Concluding Remarks

The data reviewed here for inorganic systems in solution demonstrate that transient vibrational spectroscopies are powerful tools for elucidating the electronic and molecular structures in excited states and in photochemical intermediates. When combined and applied on various time scales, time-resolved resonance Raman and infrared spectroscopies add significantly to the information available to inorganic photochemists.

Continuing developments in instrumentation will have an important influence on future studies in this area. As one example, time-resolved, step-scan FTIR spectroscopy for transient experiments on the nanosecond time scale has not only simplified data collection but has also made it possible to collect data throughout the middle-infrared region (400−4000 cm^{-1}). Transient infrared studies will no longer be limited to complexes containing carbonyl or cyanide ligands. Results are beginning to appear for nanosecond TRIR studies in the fingerprint region. Additionally, continued application of ultrafast infrared and Raman spectroscopies will open new opportunities for studying fundamental processes at very early times. Because of their sensitivity to structural changes, these spectroscopies can provide unprecedented insight into early time events. An important use of these techniques has been and will continue to be to elucidate the role of structure and to identify transients in photochemical-electron and energy-transfer processes occurring in inorganic-based molecular assemblies. When combined with transient absorption and emission measurements, these spectroscopies provide a way to acquire the broad range of experimental information required to answer detailed questions about various mechanisms and structures.

VII. Acknowledgments

The authors wish to thank Drs. Andy Shreve, Brian Dyer, Woody Woodruff, T. J. Meyer, and Carlo Bignozzi for their input and collaborations. We also wish to acknowledge support from the Laboratory Directed Research and Development Program and the Chemical Science and Technology Division at Los Alamos National Laboratory.

VIII. Abbreviations and Acronyms

4,4′-$(CO_2H)_2$bpy	4,4′-$(CO_2H)_2$-2,2′-bipyridine
4,4′-$(NH_2)_2$)bpy	4,4′-diamino-2,2′-bipyridine
4,4′-bpy	4,4′-bipyridine
4,4′-Ph_2bpy	4,4′-diphenyl-2,2′-bipyridine
4-Acpy	4-acetylpyridine
4-CNpy	4-cyanopyridine
4-Etpy	4-ethylpyridine
4-Mepy	4-methylpyridine
5,5′-dmb	5,5′-dimethyl-2,2′-bipyridine
5-mmb	5-methyl-2,2′-bipyridine
AB	2,2′:3′2″:6″,2‴-quaterpyridine
acac	acetylacetonate
Anq	anthraquinone
b	1,3-diisocyanopropane
bbpe	bis(4′-methyl-2,2′-bipyrid-4-yl)ethane
BIQ	2,2′-biquinoline
bpm	2,2′bipyrimidine
bpt	3,5-bis(pyridin-2-yl)-1,2,4-triazole
bpy	2,2′-bipyridine
bpz	2,2′-bipyrazine
CCD	charge-coupled device
Cp*	η_5-$C_5(CH_3)_5$
CT	charge transfer
CW	continuous wave
dcb	4,4′-dicarboxy-2,2′-bipyridine
dmb	4,4′-dimethyl-2,2′-bipyridine
DMCH	6,7-dihydro-5,8-dimethyldibenzo[*b*,*j*][1,10]-phenanthroline
dmp	2,9-dimethyl-1,10-phenanthroline
dpp	2,9-diphenyl-1,10-phenanthroline
dpphen	4,7-diphenyl-1,10-phenanthroline
dppm	bis(diphenylphosphino)methane
dppz	dipyrido[3,2-*a*:2′,3′-*c*]phenazine
EFFF	energy-factored force field
FTIR	Fourier transform infrared
^{i}Pr-DAB	*N*,*N*′-diisopropyl-1,4-diazobutadiene
LC	ligand centered
LF	ligand field
LMCT	ligand-to-metal charge transfer
m	4′-methyl-2,2′-bipyridyl-4′-carbonyl
Me_2phen	4,7-dimethyl-1,10-phenanthroline
Mebpy	4-methyl-2,2′-bipyridine
MLCT	metal-to-ligand charge transfer
MQ^+	*N*-methyl-4,4′-bipyridinium cation or monoquat
ns	nanosecond
OMA	optical multichannel analyzer
phen	1,10-phenanthroline
PPh_3	triphenylphosphine

py-PTZ	10-4-picol-4-ylphenothiazine
pypz	2-2-pyrid-2-ylpyrazine
RR	resonance Raman
tmp	4,4′,5,5′-tetramethyl-2,2′-bipyridine
TR^3	time-resolved resonance Raman
TRIR	time-resolved infrared
XLCT	halide-to-ligand charge transfer

IX. References

(1) Morris, D. E.; Woodruff, W. H. In *Spectroscopy of Inorganic-Based Materials*; Clark, R. J. H., Hester, R. E., Eds.; John Wiley & Sons: New York, 1987.
(2) (a) Palmer, R. A. *Spectroscopy* **1993**, *8*, 26. (b) Weidlich, O.; Siebert, F. *Appl. Spectrosc.* **1993**, *47*, 1394. (c) Murphey, R. E.; Cook, F. H.; Sakai, H. *J. Opt. Soc. Am.* **1975**, *65*, 600.
(3) (a) Turner, J. J.; George, M. W.; Johnson, F. P. A.; Westwell, J. R. *Coord. Chem. Rev.* **1993**, *125*, 101. (b) George, M. W.; Poliakoff, M.; Turner, J. J. *Analyst* **1994**, *119*, 551. (c) Turner, J. J.; Poliakoff, M. *Polyhedron* **1989**, *8*, 1637. (d) Ford, P. C.; Bridgewater, J. S.; Lee, B. *J. Photochem. Photobiol.* **1997**, *65*, 57.
(4) Kramers, H. A.; Heisenberg, W. *Z. Phys.* **1925**, *31*, 681.
(5) Dirac, P. A. M. *Proc. R. Soc. London* **1927**, *144*, 710.
(6) Albrecht, A. C.; Hutley, M. C. *J. Chem. Phys.* **1971**, *55*, 4438.
(7) (a) Heller, E. J. *Acc. Chem. Res.* **1981**, *14*, 368. (b) Heller, E. J.; Sundberg, R. L.; Tannor, D. J. *J. Phys. Chem.* **1982**, *86*, 1822.
(8) (a) Wilbrandt, R. *Biospectroscopy* **1996**, *2*, 263. (b) Wilbrandt, R.; Jensen, N. H.; Pagsberg, P.; Sillesen, A. H.; Hansen, K. B. *Nature* **1978**, *276*, 167. (c) Dallinger, R. F.; Woodruff, W. H. J. *Am. Chem. Soc.* **1979**, *101*, 4391.
(9) (a) *Ultrafast Phenomena IX*; Barbara, P. F., Ed.: Springer-Verlag: Berlin, 1994; p 1976. (b) Simon, J. D. *Rev. Sci. Instrum.* **1989**, *60*, 3597. (c) Squir, J.; Mourou, G. *Laser Focus World* **1992**, *28*, 51.
(10) Delhay, M. *Lasers in Physical Chemistry and Biophysics*; Elsevier: Amsterdam, 1975; p 213.
(11) (a) Gustafson, T. L.; Roberts, D. M.; Chernoff, D. A. *J. Chem. Phys.* **1983**, *79*, 1559. (b) Hopkins, J. B.; Renzepis, P. M. *Chem. Phys. Lett.* **1986**, *124*, 79. (c) Atkinson, G. H.; Brack, T. L.; Blanchard, D.; Rumbles, G. *Chem. Phys.* **1989**, *131*, 1. (d) Reid, P. J.; Doig, S. J.; Mathies, R. A. *Chem. Phys. Lett.* **1989**, *156*, 163. (e) Iwata, K.; Hamaguchi, H. *Chem. Phys. Lett.* **1992**, *196*, 462. (f) Petrich, J. W.; Martin, J. L. *Chem. Phys.* **1989**, *131*, 31.
(12) (a) Iwata, K.; Yamaguchi, S.; Hamaguchi, H. *Rev. Sci. Instrum.* **1993**, *64*, 2140. (b) Tahara, T.; Hamaguchi, H. *Appl. Spectrosc.* **1993**, *47*, 391.
(13) (a) Stoutland, P. O.; Dyer, R. B.; Woodruff, W. H. *Science* **1992**, *257*, 1913. (b) Hochstrasser, R. M.; Anfinrud, P. A.; Diller, R.; Han, C.; Iannone, M.; Lian, T.; Locke, B. In *Ultrafast Phenomena VII*; Harris, C. B., Ed.; Springer-Verlag: Berlin, 1990; p 229. (c) Moore, J. N.; Hansen, P. A.; Hochstrasser, R. M. *Chem. Phys. Lett.* **1987,** *138*, 110. (d) Jedju, T. M.; Robinson, M. W.; Rothberg, L. *Appl. Opt.* **1992**, *31*, 2684.
(14) (a) Hermann, H.; Grevels, F. W.; Henne, A.; Schaffner, K. *J. Phys. Chem.* **1982**, *86*, 5151. (b) Yuzawa, T.; Kato, C.; George, M. W.; Hamaguchi, H. *Appl. Spectrosc.* **1994**, *48*, 684.
(15) Palmer, R. A.; Chao, J. L.; Dittmar, R. M.; Gregoriou, V. G.; Plunkett, S. E. *Appl. Spectrosc.* **1993**, *47*, 1297.
(16) Schoonover, J. R.; Strouse, G. F.; Omberg, K. M.; Dyer, R. B. *Comments Inorg. Chem.* **1996**, *18*, 165.
(17) Schoonover, J. R.; Dyer, R. B.; Strouse, G. F.; Bates, W. D.; Chen, P.; Meyer, T. J. *Inorg. Chem.* **1996**, *35*, 273.
(18) Bradley, P. G.; Kress, N.; Hornberger, B. A.; Dallinger, R. F.; Woodruff, W. H. *J. Am. Chem. Soc.* **1981**, *103*, 744.
(19) Forster, M.; Hester, R. E. *Chem. Phys. Lett.* **1981**, *81*, 42.
(20) (a) Strommen, D. P.; Mallick, P. K.; Danzer, G. D.; Lumpkin, R. S.; Kincaid, J. R. *J. Phys. Chem.* **1990**, *94*, 1357. (b) Mallick, P. K.; Danzer, G. D.; Strommen, D. P.; Kincaid, J. R. *J. Phys. Chem.* **1988**, *92*, 5628.
(21) (a) McClanahan, S. F.; Dallinger, R. F.; Holler, F. J.; Kincaid, J. R. *J. Am. Chem. Soc.* **1985**, *107*, 4853. (b) Mabrouk, P. A.; Wrighton, M. S. *Inorg. Chem.* **1986**, *25*, 526.
(22) (a) Kumar, C. V.; Barton, J. K.; Gould, I. R.; Turro, N. J.; Houton, J. V. *Inorg. Chem.* **1988**, *27*, 648. (b) Kumar, C. V.; Barton, J. K.; Turro, N. J.; Gould, I. R. *Inorg. Chem.* **1987**, *26*, 1455.
(23) (a) Danzer, G. D.; Bajdor, K.; Kincaid, J. R. *J. Raman Spectrosc.* **1993**, *24*, 357. (b) Danzer, G. D.; Kincaid, J. R. *J. Phys. Chem.* **1990**, *94*, 3976.
(24) Strouse, G. F.; Anderson, P. A.; Schoonover, J. R.; Meyer, T. J.; Keene, F. R. *Inorg. Chem.* **1992**, *31*, 3004.
(25) (a) Carroll, P. J.; Brus, L. E. *J. Am. Chem. Soc.* **1987**, *109*, 7613. (b) Yabe, T.; Anderson, D. R.; Orman, L. K.; Chang, Y. J.; Hopkins, J. B. *J. Phys. Chem.* **1989**, *93*, 2302.
(26) (a) Chang, Y. J.; Xu, X.; Yabe, T.; Yu, S.-C.; Anderson, D. R.; Orman, L. K.; Hopkins, J. B. *J. Phys. Chem.* **1990**, *94*, 729. (b) Yabe, T.; Orman, L. K.; Anderson, D. R.; Yu, S.-C.; Xu, X.; Hopkins, J. B. *J. Phys. Chem.* **1990**, *94*, 7128.
(27) Caswell, D. S.; Spiro, T. G. *Inorg. Chem.* **1987**, *26*, 18.
(28) Turro, N. J.; Barton, J. K.; Tomalia, D. A. *Acc. Chem. Res.* **1991**, *24*, 332.
(29) (a) Somasundaran, P.; Kunjappu, J. T.; Kumar, C. V.; Turro, N. J.; Barton, J. K. *Langmuir* **1989**, *5*, 215. (b) Kunjappu, J. T.; Somasundaran, P.; Turro, N. J. *Chem. Phys. Lett.* **1989**, *162*, 233.
(30) Barton, J. K. *Comments Inorg. Chem.* **1985**, *3*, 32.
(31) Turro, C.; Bossmann, S. H.; Leroi, G. E.; Barton, J. K.; Turro, N. J. *Inorg. Chem.* **1994**, *33*, 1344.
(32) (a) Turro, C.; Bossmann, S. H.; Jenkins, Y.; Barton, J. K.; Turro, N. J. *J. Am. Chem. Soc.* **1995**, *117*, 9026. (b) Coates, C. G.; Jacquet, L.; McGarvey, J. J.; Bell, S. E. J.; Al-Obaidi, A. H. R.; Kelly, J. M. *J. Chem. Soc., Chem. Commun.* **1996**, 35.
(33) Amouyal, E.; Mouallem-Bohout, M.; Calzaferri, G. *J. Phys. Chem.* **1991**, *95*, 7641.
(34) Schoonover, J. R.; Bates, W. D.; Meyer, T. J. *Inorg. Chem.* **1995**, *34*, 6421.
(35) Strouse, G. F.; Schoonover, J. R.; Duesing, R.; Boyde, S.; Jones, W. E., Jr.; Meyer, T. J. *Inorg. Chem.* **1995**, *34*, 473.
(36) Danzer, G. D.; Golus, J. A.; Kincaid, J. R. *J. Am. Chem. Soc.* **1993**, *115*, 8643.
(37) (a) Treffertziemelis, S. M.; Golus, J. A.; Strommen, D. P.; Kincaid, J. R. *Inorg. Chem.* **1993**, *32*, 3890. (b) Treffertziemelis, S. M.; Kincaid, J. R. *J. Raman Spectrosc.* **1994**, *25*, 893.
(38) (a) Sutin, N.; Cruetz, C. *Pure Appl. Chem.* **1980**, *52*, 2717. (b) Gray, H. B.; Maverick, A. W. *Science* **1981**, *214*, 1201. (c) Kavarnos, G. J.; Turro, N. J. *Chem. Rev.* **1986**, *86*, 401.
(39) Berger, R. M.; McMillin, D. R.; Dallinger, R. F. *Inorg. Chem.* **1987**, *26*, 3802.
(40) McGarvey, J. J.; Bell, S. E.; Gordon, K. C. *Inorg. Chem.* **1988**, *27*, 4003.
(41) Gordon, K. C.; McGarvey, J. J. *Inorg. Chem.* **1991**, *30*, 2986.
(42) Al-Obaidi, A. H. R.; Gordon, K. C.; McGarvey, J. J.; Bell, S. E. J.; Grimshaw, J. *J. Phys. Chem.* **1993**, *97*, 10942.
(43) (a) Cotton, F. A.; Walton, R. A. *Multiple Bonds Between Metal Atoms*, 2nd ed.; Clarendon Press: Oxford, 1993. (b) Cotton, F. A.; Walton, R. A. *Struct. Bonding (Berlin)* **1985**, *62*, 1. (c) Poli, R. *Comments Inorg. Chem.* **1992**, *12*, 285.
(44) Dallinger, R. F. *J. Am. Chem. Soc.* **1985**, *107*, 7202.
(45) Schoonover, J. R.; Dallinger, R. F.; Killough, P. M.; Sattleberger, A. P.; Woodruff, W. H. *Inorg. Chem.* **1991**, *30*, 1093.
(46) Smith, D. C.; Gray, H. B. *Coord. Chem. Rev.* **1990**, *100*, 169.
(47) Dallinger, R. F.; Miskowski, V. M.; Gray, H. B.; Woodruff, W. H. *J. Am. Chem. Soc.* **1981**, *103*, 1595.
(48) Doorn, S. K.; Gordon, K. C.; Dyer, R. B.; Woodruff, W. H. *Inorg. Chem.* **1992**, *31*, 2284.
(49) Harvey, P. D.; Dallinger, R. F.; Woodruff, W. H.; Gray, H. B. *Inorg. Chem.* **1989**, *28*, 3057.
(50) Ishitani, O.; George, M. W.; Ibusuki, T.; Johnson, F. P. A.; Koike, K.; Nozaki, K.; Pac, C.; Turner, J. J.; Westwell, J. R. *Inorg. Chem.* **1994**, *33*, 4712, 4717.
(51) Dougherty, T. P.; Grubbs, W. T.; Heilweil, E. J. *J. Phys. Chem.* **1994**, *98*, 9396.
(52) (a) Wrighton, M. S.; Morse, D. L. *J. Am. Chem. Soc.* **1974**, *96*, 998. (b) Luong, J. C.; Nadjo, L.; Wrighton, M. S. *J. Am. Chem. Soc.* **1978**, *100*, 5790. (c) Stufkens, D. J. *Comments Inorg. Chem.* **1992**, *13*, 359 and references therein.
(53) (a) Hawecker, J.; Lehn, J. M.; Ziessel, R. *J. Chem. Soc., Chem. Commun.* **1984**, 328. (b) Sullivan, B. P.; Bolinger, M. C.; Conrad, D.; Vining, W. J.; Meyer, T. J. *J. Chem. Soc., Chem. Commun.* **1985**, 1414. (c) Hawecker, J.; Lehn, J. M.; Ziessel, R. *Helv. Chim. Acta* **1986**, *69*, 1990. (d) Breikss, A. J.; Abruña, H. D. *J. Electroanal. Chem. Interfacial Electrochem.* **1986**, *201*, 353.
(54) (a) Juris, A.; Campagna, S.; Bidd, I.; Lehn, J. M.; Ziessel, R. *Inorg. Chem.* **1988**, *27*, 4007. (b) Kaim, W.; Kramer, H. E. A.; Bogler, C.; Reiker, J. *J. Organomet. Chem.* **1989**, *107*, 367. (c) Kalyanasundaram, K. *J. Chem. Soc., Faraday Trans.* **1986**, *2*, 2401. (d) Casper, J. V.; Meyer, T. J. *J. Phys. Chem.* **1983**, *87*, 952.
(55) (a) Westmoreland, T. D.; Schanze, K. S.; Neveux, P. E.; Danielson, E.; Sullivan, B. P.; Chen, P.; Meyer, T. J. *Inorg. Chem.* **1985**, *24*, 2596. (b) Chen, P.; Danielson, E.; Meyer, T. J. *J. Phys. Chem.* **1988**, *92*, 3708. (c) Chen, P.; Westmoreland, T. D.; Danielson, E.; Schanze, K. S.; Anthon, D.; Neveux, P.; Meyer, T. J. *Inorg. Chem.* **1987**, *26*, 1116. (d) Worl, L. A.; Duesing, R.; Chen, P.; Della Ciana, L.; Meyer, T. J. *J. Chem. Soc., Dalton Trans.* **1991**, 849.
(56) Sullivan, B. P. *J. Phys. Chem.* **1989**, *93*, 24.
(57) (a) Chen, P.; Mecklenburg, S. L.; Duesing, R.; Meyer, T. J. *J. Phys. Chem.* **1993**, *97*, 6811. (b) Chen, P.; Duesing, R.; Graff, D. K.; Meyer, T. J. *J. Phys. Chem.* **1991**, *95*, 5850. (c) Chen, P.; Duesing, R.; Tapolsky, G.; Meyer, T. J. *J. Am. Chem. Soc.* **1989**, *111*, 8305. (d) MacQueen, D. B.; Schanze, K. S. *J. Am. Chem. Soc.* **1991**, *113*, 7470.
(58) (a) Drickamer, H. G.; Salman, O. A. *J. Chem. Phys.* **1982**, *77*, 3337. (b) Reitz, G. A.; Dressick, W. J.; Demas, J. N.; Degraff, B.

A. *J. Am. Chem. Soc.* **1986**, *108*, 5344. (c) Reitz, G. A.; Demas, J. N.; Degraff, B. A. *J. Am. Chem. Soc.* **1988**, *110*, 5051.
(59) (a) Shaw, J. R.; Schmehl, R. H. *J. Am. Chem. Soc.* **1991**, *113*, 389. (b) Leasure, R. M.; Sacksteder, L.; Nesselrodt, D.; Reitz, G. A.; Demas, J. N.; DeGraff, B. A. *Inorg. Chem.* **1991**, *30*, 3722. (c) Sacksteder, L.; Zipp, A. P.; Brown, E. A.; Streich, J.; Demas, J. N.; Degraff, B. A. *Inorg. Chem.* **1990**, *29*, 4335. (d) Juris, A.; Campagna, I. B.; Lehn, J. L.; Ziessel, R. *Inorg. Chem.* **1988**, *27*, 4007. (e) Fredericks, S. M.; Luong, J. C.; Wrighton, M. S. *J. Am. Chem. Soc.* **1979**, *101*, 7415. (f) Giordano, P. J.; Wrighton, M. S. *J. Am. Chem. Soc.* **1979**, *101*, 2889.
(60) (a) Glyn, P.; George, M. W.; Hodges, P. M.; Turner, J. J. *J. Chem. Soc., Chem. Commun.* **1989**, 1655. (b) Gamelin, D. R.; George, M. W.; Glyn, P.; Grevels, F. W.; Johnson, F. P. A.; Klotzbücher, W.; Morrison, S. L.; Russel, G.; Schaffner, K.; Turner, J. J. *Inorg. Chem.* **1994**, *33*, 3246.
(61) (a) Schoonover, J. R.; Gordon, K. C.; Argazzi, R.; Woodruff, W. H.; Peterson, K. A.; Bignozzi, C. A.; Dyer, R. B.; Meyer, T. J. *J. Am. Chem. Soc.* **1993**, *115*, 10996. (b) George, M. W.; Johnson, F. P. A.; Westwell, J. R.; Hodges, P. M.; Turner, J. J. *J. Chem. Soc., Dalton Trans.* **1993**, 2927. (c) Rossenaar, B. D.; George, M. W.; Johnson, F. P. A.; Stufkens, D. J.; Turner, J. J.; Vlcek, A., Jr. *J. Am. Chem. Soc.* **1995**, *117*, 11582.
(62) Schoonover, J. R.; Strouse, G. F.; Chen, P.; Bates, W. D.; Meyer, T. J. *Inorg. Chem.* **1993**, *32*, 2618.
(63) George, M. W.; Johnson, F. P.; Turner, J. J.; Westwell, J. R. *J. Chem. Soc., Dalton Trans.* **1995**, 2711.
(64) Morrison, S. L.; Turner, J. J. *J. Mol. Struct.* **1994**, *317*, 39.
(65) Strouse, G. F.; Gudel, H. U. *Inorg. Chim. Acta* **1995**, *240*, 453.
(66) Strouse, G. F.; Gudel, H. U.; Bertolasi, V.; Ferretti, V. *Inorg. Chem.* **1995**, *34*, 5578.
(67) Perng, J.-H.; Zink, J. I. *Inorg. Chem.* **1990**, *29*, 1158.
(68) (a) Johnson, F. P.; George, M. W.; Turner, J. J. *Inorg. Chem.* **1993**, *32*, 4226. (b) Glyn, P.; George, M. W.; Lees, A.; Turner, J. J. *Inorg. Chem.* **1991**, *30*, 3542.
(69) Johnson, F. P.; George, M. W.; Turner, J. J.; Morrison, S. L. *J. Chem. Soc., Chem. Commun.* **1995**, 391.
(70) Tutt, L.; Zink, J. I. *J. Am. Chem. Soc.* **1986**, *108*, 5830.
(71) George, M. W.; Turner, J. J.; Westwell, J. R. *J. Chem. Soc., Dalton Trans.* **1994**, 2217.
(72) McNicholl, R. A.; McGarvey, J. J.; Al-Obaidi, A. H. R.; Bell, S. E. J.; Jayaweera, P. M.; Coates, C. G. *J. Phys. Chem.* **1995**, *99*, 12268.
(73) (a) Rooney, A. D.; McGarvey, J. J.; Gordon, J. C. *Organometallics* **1995**, *14*, 107. (b) Bell, S.; Gordon, K. C.; McGarvey, J. J. *J. Am. Chem. Soc.* **1988**, *110*, 3107.
(74) Nieuwenhuis, H. A.; Stufkens, D. J.; McNicholl, R. A.; Al-Obaidi, A. H. R.; Coates, C. G.; Bell, S. E. J.; McGarvey, J. J.; Westwell, J.; George, M. W.; Turner, J. J. *J. Am. Chem. Soc.* **1995**, *117*, 5579.
(75) (a) Creutz, C.; Sutin, N. *Proc. Natl. Acad. Sci. U.S.A.* **1975**, *72*, 2858. (b) Young, R. C.; Meyer, T. J.; Whitten, D. G. *J. Am. Chem. Soc.* **1975**, *97*, 4782. (c) Lin, C.-T.; Sutin, N. *J. Phys. Chem.* **1976**, *80*, 97. (d) Kalyanasundaram, K. *Coord. Chem. Rev.* **1982**, *46*, 159. (e) Sutin, N.; Creutz, C. *Pure Appl. Chem.* **1980**, *52*, 2717. (f) Whitten, D. G. *Acc. Chem. Res.* **1978**, *11*, 94. (g) Meyer, T. J. *Acc. Chem. Res.* **1978**, *11*, 94. (h) Balzani, V.; Moggi, L.; Manfrin, M. F.; Bolletta, F.; Gleria, M. *Science* **1975**, *189*, 852. (i) Elliott, C. M.; Freitag, R. A.; Blaney, D. D. *J. Am. Chem. Soc.* **1985**, *107*, 4647. (j) Elliott, C. M.; Freitag, R. A. *J. Chem. Soc., Chem. Commun.* **1985**, 156. (k) Westmoreland, T. D.; Le Bozec, H.; Murray, R. W.; Meyer, T. J. *J. Am. Chem. Soc.* **1983**, *105*, 5952. (l) Matsuo, T.; Skamoto, T.; Takuma, K.; Sakura K.; Ohsako, T. *J. Phys. Chem.* **1981**, *85*, 1277.
(76) (a) Scandola, F.; Indelli, M. T.; Chiorboli, C.; Bignozzi, C. A. *Top. Current Chem.* **1990**, *158*, 75. (b) *Photoinduced Electron Transfer*; Chanon, M., Fox, M. A., Eds.; Elsevier: New York, 1988 and references therein.
(77) (a) Mabrouk, P. A.; Wrighton, M. S. *Spectrochim. Acta* **1989**, *45A*, 17. (b) Vauthey, E.; Phillips, D.; Parker, A. W. *J. Phys. Chem.* **1992**, *96*, 7356.
(78) (a) McMahon, R. J.; Force, R. K.; Patterson, H. H.; Wrighton, M. S. *J. Am. Chem. Soc.* **1988**, *110*, 2670. (b) Force, R. K.; McMahon, R. J.; Yu, J.; Wrighton, M. S. *Spectrochim. Acta* **1989**, *45A*, 23.
(79) Schoonover, J. R.; Chen, P.; Bates, W. D.; Dyer, R. B.; Meyer, T. J. *Inorg. Chem.* **1994**, *33*, 793.
(80) Strouse, G. F.; Schoonover, J. R.; Duesing, R.; Meyer, T. J. *Inorg. Chem.* **1995**, *34*, 2725.
(81) (a) Mecklenburg, S. L.; Peek, B. M.; Schoonover, J. R.; McCafferty, D. G.; Wall, C. G.; Erickson, B. W.; Meyer, T. J. *J. Am. Chem. Soc.* **1993**, *115*, 5479. (b) Mecklenburg, S. L.; McCafferty, D. G.; Schoonover, J. R.; Peek, B. M.; Erickson, B. W.; Meyer, T. J. *Inorg. Chem.* **1994**, *33*, 2974.
(82) (a) Woiteller, S.; Launay, J. P.; Joachim, C. *Chem. Phys.* **1989**, *131*, 481. (b) Mikkelsen, K. V.; Ratner, M. A. *J. Phys. Chem.* **1989**, *93*, 1759. (c) Kuznets, A. M.; Ulstrup, J. *J. Chem. Phys.* **1981**, *75*, 2047. (d) Uzer, T.; Hynes, J. T. *J. Phys. Chem.* **1986**, *90*, 3524. (e) Schipper, P. E. *J. Phys. Chem.* **1986**, *90*, 2351. (f) Piepho, S. B.; Krausz, E. R.; Schatz, P. N. *J. Am. Chem. Soc.* **1978**, *100*, 2996. (g) Wong, K. Y.; Schatz, P. N.; Piepho, S. B. *J. Am. Chem. Soc.* **1979**, *101*, 2793.
(83) (a) Wacholtz, W. F.; Auerbach, R. A.; Schmehl, R. S. *Inorg. Chem.* **1986**, *25*, 227. (b) Balzani, V.; Barigelletti, F.; Campagna, S.; Belser, P.; von Zelewsky, A. *Coord. Chem. Rev.* **1988**, *84*, 85. (c) Murphy, W. R., Jr.; Brewer, K. T.; Petersen, J. D. *Inorg. Chem.* **1987**, *26*, 3376. (d) Fuchs, Y.; Lofters, S.; Dieter, T.; Shi, W.; Morgan R.; Strekas, T. C.; Gafney, H. D.; Baker, A. D. *J. Am. Chem. Soc.* **1987**, *109*, 2691. (e) Nishizawa, M.; Ford, P. C. *Inorg. Chem.* **1981**, *20*, 2016. (f) Rumininski, R. R.; Cockroft, T.; Shoup, M. *Inorg. Chem.* **1988**, *27*, 4026. (g) Braunstein, H. C.; Baker, D. A.; Strekas, T. C.; Gafney, D. H. *Inorg. Chem.* **1984**, *23*, 857. (h) Rumininski, R. R.; Kiplinger J.; Cockroft, T.; Chase, C. *Inorg. Chem.* **1989**, *28*, 370. (i) Curtis, J. C.; Bernstein, J. S.; Meyer, T. J. *Inorg. Chem.* **1985**, *24*, 385.
(84) (a) Ward, M. D. *J. Chem. Soc., Dalton Trans.* **1993**, 1321. (b) Ward, M. D. *J. Chem. Soc., Dalton Trans.* **1994**, 3095. (c) Bardwell, D. A.; Barigelletti, F.; Cleary, R. L.; Flamigni, L.; Guardegli, M.; Jeffery, J. C.; Ward, M. D. *Inorg. Chem.* **1995**, *34*, 2438.
(85) Hughes, H. P.; Martin, D.; Bell, S.; McGarvey, J. J.; Vos, J. G. *Inorg. Chem.* **1993**, *32*, 4402.
(86) Indelli, M. T.; Bignozzi, C. A.; Harriman, A.; Schoonover, J. R.; Scandola, F. *J. Am. Chem. Soc.* **1994**, *116*, 3768.
(87) Bignozzi, C. A.; Argazzi, R.; Chiorboli, C.; Scandola, F.; Dyer, R. B.; Schoonover, J. R.; Meyer, T. J. *Inorg. Chem.* **1994**, *33*, 3..
(88) Bignozzi, C. A.; Argazzi, R.; Garcia. C. G.; Scandola, F.; Schoonover, J. R.; Meyer, T. J. *J. Am. Chem. Soc.* **1992**, *114*, 8727.
(89) Bignozzi, C. A.; Argazzi R.; Schoonover, J. R.; Gordon, K. C.; Dyer, R. B.; Scandola, F. *Inorg. Chem.* **1992**, *31*, 5260.
(90) Doorn, S. K.; Stoutland, P. O.; Dyer, R. B.; Woodruff, W. A. *J. Am. Chem. Soc.* **1992**, *114*, 3133.
(91) Turro, N. J.; Kumar, C. V.; Grauer, Z.; Barton, J. K. *Langmuir* **1987**, *3*, 1056.
(92) (a) Incavo, J. A.; Dutta, P. K. *J. Phys. Chem.* **1990**, *94*, 3075. (b) Ledney, M.; Dutta, P. K. *J. Am. Chem. Soc.* **1995**, *117*, 7687.
(93) Maruszewski K.; Strommen, D. P.; Kincaid, J. R. *J. Am. Chem. Soc.* **1993**, *115*, 8345.
(94) Dutta, P. K.; Tuberville, W. *J. Phys. Chem.* **1992**, *96*, 9410, 9416.

CR950273Q